Thermochemical Processes for the Production of Hydrogen from Water

James E. Funk

College of Engineering
University of Kentucky
Lexington, Kentucky 40506

Introduction

A thermochemical hydrogen production process is one which requires only (i.e. mainly) water as a material input and mainly thermal energy, or heat, as an energy input. The output of the process is hydrogen and oxygen and possibly (or probably) some waste heat. The process itself comprises a series of chemical reactions which sum to water decomposition. The products of each reaction must be separated and either recycled or sent to the next reaction. Thermal energy, or heat, is transferred in the process to heat or cool the various reactant and product streams and to provide for the various "heats of reaction." Useful work, or electricity, will be required for pumping and/or operating separation equipment or electrochemical reactions. A "pure" thermochemical process requires only heat as the energy input. A "hybrid" process is one which contains an electrochemical step. In water electrolysis, 80% of the energy input must be in the form of electricity.

The interest in thermochemical processes derives from the potential they offer for lower capital and/or operating costs and higher overall thermal efficiency than water electrolysis. Water electrolysis has been used for some time as an industrial process to produce hydrogen and is especially attractive in areas where electricity is abundant and inexpensive. The thermal efficiency - measured from primary thermal energy source to hydrogen in the pipeline - of the water electrolysis process is in the range of 30-35%. The major determinant is the efficiency of converting heat to useful work (i.e. electricity) which is currently in the range of 35-40%.

The definition of thermal efficiency, η, used here is

$$\eta = \frac{\Delta H_o}{Q_t} \qquad 1)$$

where

$$Q_t = q_i + \frac{W_i}{\varepsilon} \qquad 2)$$

where ΔH_o = enthalpy change upon decomposition of liquid water to hydrogen and oxygen at 25° C and 1 atm. (68.3 kcal/g mole H_2)

Q_t = total thermal energy required by the process

q_i = direct thermal energy input

w_i = direct useful work input

ε = efficiency of converting thermal energy to useful work

This definition of η employs the so-called "higher heating value" of hydrogen, but the motivation for its use springs from the fact that liquid water will, in fact, be the material input to the process. End use considerations should not be important in a definition which is meant to focus on the process, as has been argued earlier (1).

This research is supported by NASA-Lewis Grant No. NGR 18-001-086

The first paper dealing with the energetics and thermodynamics of thermochemical processes for the decomposition of water was published in 1966 (2). The number of publications on this subject grew rapidly after 1971 with the emergence of an intense worldwide interest in a possible hydrogen economy. The proceedings of The Hydrogen Economy Miami Energy (THEME) Conference (3) contain papers on virtually every aspect of a hydrogen economy including several on thermochemical processing. Two recent review articles, by Braunstein & Bamberger (4) and Chao (5), and a number of other recent papers (6-15) present detailed technical discussions of many aspects of the problem and a long list of references.

Efficiency

Costs, capital and operating, will undoubtedly play the major role in determining what sort of hydrogen production processes become widely used in the future. Thermal efficiency, however, will exert a strong influence on costs and is a reasonable measure to use in the search for "good" thermochemical processes.

The thermodynamic limitation on thermal efficiency, first published in 1966 (2), and verified several times since then, is

$$\eta \leq \left\{ \begin{array}{l} \dfrac{1}{1 + \dfrac{q_r}{\Delta H_o} + \left(\dfrac{W_i}{\Delta H_o} \; \dfrac{1-\varepsilon}{\varepsilon} \right)} \\ \\ \dfrac{\Delta H_o}{\Delta G_o} \; \dfrac{T_H - T_c}{T_H} \left[\dfrac{1}{1 + \dfrac{1}{\varepsilon} \; \dfrac{W_i}{\Delta G_o} \left(\dfrac{T_H - T_c}{T_H} - \varepsilon \right)} \right] \end{array} \right. \qquad 3)$$

The derivation leading to this result employs the assumption that all the process thermal energy input, q_i, occurs at the high temperature, T_H, and that all the process heat rejection, q_r, takes place at the heat sink temperature, T_c. ΔG_o is the change in the Gibbs function upon decomposition of liquid water to hydrogen and oxygen at 25° C and 1 atm. (56.7 kcal/g mole H_2).

Equation (3) fixes the upper limit on η (when q_r and W_i are = 0) such that

$$\eta \leq \left\{ \begin{array}{l} 1.0 \\ \\ \dfrac{\Delta H_o}{\Delta G_o} \; \dfrac{T_H - T_c}{T_H} \end{array} \right. \qquad 4)$$

It should be pointed out here that the upper limit on η shown in Equation 4 is 1.0 because it was assumed that q_r, the process heat rejection, could not be negative. If this restriction is removed, which would allow heat to flow into the process from the heat sink at T_c, the upper limit will be given by the lower expression in Equation 4 and will approach 1.2 (i.e. $\Delta H_o/\Delta G_o$), which is exactly the situation for water electrolysis when the process efficiency is based on the "thermoneutral" voltage.

Single Stage Process

The simplest single step process to decompose water is electrolytic. Actual operating data (16) indicate that water electrolysis cells consume 20-27 kw-hr/lb of H_2 generated. The cell efficiency, based on a ΔH_o of 18.1 kw-hr/lb H_2, is then in the range 66-90%. The simplest conceptual thermal process is to heat the water to a high temperature and separate the hydrogen and oxygen which form in the equilibrium mixture.

The entropy change for water decomposition, after the liquid to vapor phase change has occurred, is approximately 0.01 kcal/g mole °K which is simply too small to achieve a substantial reduction in the work requirement at currently achievable operating temperatures. Another way of saying this is that the equilibrium composition does not shift in favor of H_2 rapidly enough with increasing temperature to suggest that a single step thermal decomposition process offers great promise for the near term. At 2000° K and 1 atm the equilibrium mixture of $H_2O - H_2 - O_2$ contains a mole fraction of H_2 equal to only 0.036 corresponding to only a 3.6% conversion of water. High temperature gas cooled reactors which may be able to provide process heat in the near future are operating in the range of 1200-1300° K (17).

In any direct decomposition process there will be severe practical problems related to the very high temperatures required. Materials of construction, heat exchangers, separation membranes and reaction vessels will present considerable difficulties, but the real and unavoidable drawback has to do with the small entropy increase for the water decomposition reaction. In a practical sense it is not possible to reduce the useful work requirement to zero.

Multistage Processes

As was shown by Funk & Reinstrom (2) and reiterated by Abraham and Schreiner in 1974 (11), it is possible for a multistage process to satisfy the first and second laws of thermodynamics along with the constraint that no useful work be expended in the process. In order to visualize such a situation one should imagine a general thermochemical process comprising an arbitrary number of steps. Each reaction exhibits some change in enthalpy, ΔH, entropy, ΔS, and Gibbs function or free energy, ΔG. If the entire process is operated reversibly at 25° C and 1 atm, the work and heat requirements will be exactly the same as for an ideal electrolysis cell since the work requirement, ΔG, and the heat requirement, $T\,\Delta S$, are the same for any and all reversible processes. In this sense the reversible constant temperature and pressure thermochemical process is the same as the reversible water electrolysis cell. The work requirement for electrolysis can be reduced by operating at higher temperatures, but by choosing the operating temperatures in the thermochemical process properly it is possible, at least in principle, to reduce the useful work requirement to zero. In the chemical process the work requirement maniifests itself mainly in work of separation required in the various reaction steps.

The total process useful work requirement may be reduced by operating some of the reactions at high temperatures and some at low temperatures. If the work requirement for the reaction step is taken to be the change in the Gibbs function for the reaction, the object is to operate those reactions with positive entropy changes at high temperatures. Neglecting the effect of temperature on enthalpy and entropy changes, and realizing that phase changes must be treated with care, the following analysis may be made.

The work and heat requirements for the ith reaction are given by

$$W_i = W_i^{T_o} - \Delta S_i \,(T_i - T_o) \qquad 5)$$

$$q_i = q_i^{T_o} + \Delta S_i \,(T_i - T_o) \qquad 6)$$

where the o subscript refers to a reference or standard temperature, say 25° C.

The effect of the sign of the reaction entropy change is apparent. The total heat and work requirements are obtained by summing, so that

$$W_T = \Delta G_o - \sum_{i=1}^{I} \Delta S_i \,(T_i - T_o) \qquad 8)$$

Now, suppose that J reactions have positive entropy changes and are operated at high temperatures, T_i and L reactions have negative entropy changes and are operated at T_o. The total work, W_T, will be zero when

$$\sum_{i=1}^{J} \Delta S_i (T_i - T_o) = \Delta G_o \qquad 9)$$

If only one high temperature, say T_H is employed, the result is

$$\sum_{i=1}^{J} \Delta S_i = \frac{\Delta G_o}{T_H - T_o} \qquad 10)$$

In principle, there is no reason why Equations 9 and 10 cannot be satisfied along with

$$\sum_{i=1}^{I} \Delta S_i = \sum_{j=1}^{J} \Delta S_j + \sum_{i=J+1}^{J+L} \Delta S_i = \Delta S_o \qquad 11)$$

This conclusion cannot be reached for a one step process. In that case, the zero work requirement must be accomplished by a temperature manipulation rather than the selection of a suitable sequence of chemical reaction.

Two-Stage Process

Suppose a two-reaction process has been found which requires no useful work. One reaction is operated at T_c and the other at T_H. Choose $T_c = 100°$ C and $T_H = 950°$ C and assume that ΔH and ΔS are independent of temperature. For the decomposition of water vapor at 100° C, $\Delta H = 58.1$, $\Delta G = 53.8$, and $\Delta S = 0.0116$, and H_2O is assumed to enter the process in the vapor phase. Since the work required is zero, $\Delta G_c = \Delta G_H = 0$ and

$$\Delta H_H = T_H \Delta S_H \qquad 12)$$

$$\Delta H_c = T_c \, \Delta S_c \qquad 13)$$

From Equation 10 it is found that

$$\Delta S_H = \frac{53.8}{950-100} = +0.0633$$

and, from Equation 12

$$\Delta H_H = (1223)\ (.0633) = +77.4$$

Since the ΔS's must sum to 0.0116

$$\Delta S_L = -0.0517$$

From Equation 13

$$\Delta H_c = (373)\ (-.0517) = -19.3$$

Abraham and Schreiner (11) indicate that the positive entropy change required for the high temperature reaction (+0.0633) is too large for real substances. Funk and Reinstrom (2) have expressed the opinion that it is unlikely that elements or simple compounds will be found to operate in efficient two-step processes. It is interesting, however, to consider processes which employ the steam-methane reforming reaction. This reaction has a very large entropy change and has been suggested by Schulten as a "good" reaction for thermochemical processes (17).

A two-step process using the steam-methane reforming reaction is shown below

Reaction	
1	$CH_4\ (g) + H_2O\ (g) \rightarrow CO\ (g) + 3H_2\ (g)$
2	$CO\ (g) + 2H_2(g) \rightarrow CH_4(g) + \frac{1}{2} O_2\ (g)$

Reaction No. 2 is shown to illustrate the point. It is not suggested here that it will "go" as written. The reaction property changes are

Reaction	Temp ° C	ΔH	ΔG	ΔS
1	100	50.2	30.1	+ 0.0541
2	100	7.9	23.7	- 0.0425
1	627	53.6	- 0.4	+ 0.0601

The ΔG for reaction 1 is zero at 621° C. Notice that the work requirement, or at least the free energy change, has been reduced by approximately 30 kcal by raising the operating temperature 527° C. The entropy change for the steam-methane reforming reaction almost satisfies the requirement mentioned earlier. The work of separation for this reaction is high, however, and this is an important quantity in thermochemical processes, as has been described elsewhere (7).

Cycle Evaluation

The complete evaluation of a thermochemical process is a complex and involved task. Experimental data on the reactions describing both equilibrium and kinetic conditions are required. Information dealing with corrosion and materials of construction should be available. Then, from a full mass and energy balance and equipment design or specification the thermal efficiency and capital and operating costs can be determined. Such effort cannot be applied, of course, to every process and an automated procedure for cycle evaluation is necessary. Such a procedure has been developed and is embodied in the HYDRGN computer program, which has been described elsewhere (1). This technique operates in conjunction with a large thermochemical data bank and a program which determines the equilibrium composition of reacting mixtures. It calculates important process conditions such as:

1. Thermodynamic property changes in each step of process, including the heating and cooling steps,
2. Amount of recycle and work of separation (for gas mixtures) as a function of the approach to equilibrium in the chemical reaction steps,
3. Possibilities for thermal energy regeneration and useful work production in the process itself, and
4. An estimate of the overall process thermal efficiency.

The output of the HYDRGN program may be used to generate more detailed mass and energy balances and may be adapted to a particular process to do parametric studies. This evaluation procedure has been widely used and applied to over 100 processes.

A Hybrid Cycle

A good example of a hybrid cycle is the so called hybrid sulfuric acid process now being developed by Westinghouse and NASA. The reactions and their standard state property changes are

Step No.		298° K, 1 atm		
		ΔH*	ΔG*	ΔS**
1	$2H_2O(l) + SO_2(g) \rightarrow H_2SO_4(l) + H_2(g)$	13.0	20.2	- .024
2	$H_2SO_4(l) \rightarrow H_2O(l) + SO_2(g) + \frac{1}{2}O_2(g)$	55.3	36.5	.063
	$H_2O(l) \rightarrow H_2(g) + \frac{1}{2}O_2(g)$	68.3	56.7	.039

* kcal/g mole H_2 ** kcal/g mole H_2° K

The first step is accomplished electrolytically and the second, the decomposition of sulfuric acid, is done thermally. Step No. 2 has a large positive entropy change, which is necessary for a good thermochemical process. The work requirement in the first step may be reduced by operating with acid concentrations less than 100%, which has the effect of shifting some of the work requirement into the second step in which thermal energy is the major input. A detailed cost and efficiency estimate has been prepared by Westinghouse and NASA and is presented elsewhere in this symposium.

A Sulfur Cycle

The large entropy changes associated with the decomposition of sulfates and/or SO_3 has led to the generation of a number of processes incorporating such a step (10, 12). One such cycle is

	ΔH*	ΔG*	ΔS**
$\frac{1}{4}BaS + H_2O \rightarrow \frac{1}{4}BaSO_4 + H_2$	7.3	1.7	.0187
$\frac{1}{4}BaSO_4 + \frac{1}{2}S \rightarrow \frac{1}{4}BaS + \frac{1}{2}SO_2$	25.6	19.1	.0217
$\frac{5}{2}SO_2 + Fe_2O_3 \rightarrow 2FeSO_4 + \frac{1}{2}S$	-69.4	-37.3	- .1075
$2FeSO_4 \rightarrow Fe_2O_3 + 2SO_2 + \frac{1}{2}O_2$	104.8	73.2	.1061
$H_2O \rightarrow H_2 + \frac{1}{2}O_2$	68.3	56.7	.039

*kcal/g mole H_2 **kcal/g mole H_2°K 298°K, 1 atm

Preliminary estimates indicate that such a cycle could have an efficiency around 40% when the maximum process temperature is 1144° K. A more detailed study is now under way.

A great deal of experimental and theoretical work is now being done by various organizations on a worldwide basis. Table 1 shows some of the processes, cast in terms of the hydrogen and oxygen producing reactions from which they proceed, and the organizations which are doing the research and development. The overall program is broad and a number of avenues - both experimental and theoretical - are being pursued. The results, obtained in the laboratory and from engineering designs, should provide the information necessary to make a realistic evaluation of the true potential of thermochemical processes.

TABLE 1

A Process Classification and Development Scheme

$$H_2O + \bigcirc \longrightarrow \square + H_2$$

$$\square \longrightarrow \bigcirc \quad 1/2\ O_2$$

	○	□	Organization
1	CH_4	$(CO+2H_2)$	KFA-Julich, West Germany Lawrence Livermore Laboratory
2	$(SO_2 + H_2O)$	H_2SO_4	Westinghouse Hybrid Sulfuric Acid KFA-Julich, West Germany Los Alamos Scientific Laboratory
3	$(3FeCl_2 + 3H_2O)$	$(Fe_3O_4 + 6HCl)$	IGT GE Euratom-Ispra, Italy RWTH-Aachen, West Germany
4	1/2 Sn	1/2 SnO_2	Gaz de France
5	1/2 S	1/2 SO_2	Los Alamos Scientific Laboratory University of Kentucky
6	$(K_2Se + H_2O)$	(2KOH + Se)	Lawrence Livermore Laboratory
7	Cl_2*	2HCl	Allison Division, GM Air Products IGT RWTH, Aachen, West Germany
8	$(2Cs + H_2O)$	2CsOH	Aerojet General
9	3FeO	Fe_3O_4	IGT RWTH, Aachen, West Germany
10	Hg	HgO	Euratom, Ispra (Mark-1)
11	1/3 KI	1/3 KIO_3	GE
12	SO_2	SO_3	IGT
13	3/4 Fe	3/4 Fe_3O_4	IGT RWTH, Aachen, West Germany
14	$(SrBr_2 + Hg)$	$(SrO + HgBr_2)$	Euratom, Ispra, Italy

---

*Reverse the $H_2 + 1/2O_2$

References

1. Funk, J. E., Conger, W. L., and Carty, R. H., "Evaluation of Multi-Step Thermochemical Processes for the Production of Hydrogen from Water," THEME Conf. Proc., Miami Beach, Fla., pp. S11-.11, March, 1974.

2. Funk, J. E. and Reinstrom, R. M., "Energy Requirements in the Production of Hydrogen from Water," I & EC Proc. Res. and Dev., Vol. 5, No. 3, pp. 336-342, July, 1966.

3. Proceedings of The Hydrogen Economy Miami Energy (THEME) Conference, University of Miami, Miami Beach, Fla., March 18-20, 1974.

4. Bamberger, C. E. and Braunstein, J., "Hydrogen: A Versatile Element," Amer. Sci., Vol. 63, No. 4, pp. 438-447, July-August, 1975.

5. Chao, R. E., "Thermochemical Water Decomposition Processes," I & EC Proc. Res. and Dev., Vol. 13, No. 2, pp. 94-101, June, 1974.

6. Marchetti, C., "Hydrogen Energy," Chemical Economy and Engineering Review, Chemical Economy Research Institute (Japan), January, 1973.

7. Funk, J. E., "Thermodynamics of Multi-Step Water Decomposition Processes," Proc. Sym. on Non-Fossil Chemical Fuels, ACS 163rd National Meeting, Boston, Mass., pp. 79-87, April, 1972.

8. Funk, J. E., "The Generation of Hydrogen by the Thermal Decomposition of Water," Proc. 9th IECEC, San Francisco, Calif., August 26-30, 1974.

9. Funk, J. E., Conger, W. L., Carty, R.M., and Barker, R.E., "Thermochemical Production of Hydrogen from Water," Proc. British Nuclear Energy Soc. Int'l. Conf. on the High Temp. Reactor and Proc. Applic., London, England, November 26-28, 1974.

10. Bowman, M. G., "Fundamental Aspects of Systems for the Thermochemical Production of Hydrogen from Water," Proc. First National Topical Meeting on Nuc. Heat Applic., Los Alamos, New Mexico, October 1-3, 1974.

11. Abraham, B. M. and Schreiner, F., "General Principles Underlying Chemical Cycles which Thermally Decompose Water into the Elements," I & EC Fund, Vol. 13, No. 4, pp. 305-310, 1974.

12. Soliman, M. A., Carty, R. H., Conger, W. L. and Funk, J. E., "New Thermochemical Cycles for Hydrogen Production," Canad. Jour. Chem. Eng., Vol. 53, pp. 164-169, April, 1975.

13. Chao, R. E., "Thermochemical Hydrogen Production: An Assessment of Nonideal Cycles," Ind. Eng. Chem. Process Des. Dev., Vol. 14, No. 3, pp. 276-279, 1975.

14. Bamberger, C. E., et al., "Thermochemical Decomposition of Water Based on Reactions of Chromium and Barium Compounds," Science, Vol. 189, pp. 715-716, Aug. 29, 1975.

15. Funk, J. E., "Thermochemical and Electrolytic Production of Hydrogen from Water," Introduction to Hydrogen Energy, T.N. Vezeroglu, Ed., Int. Assn. Hyd. Energy, pp. 19-49, Sept. 1975.

16. Michael, J. W., et al., "Hydrogen and Other Synthetic Fuels," TID 26136, UC-80, September, 1972.

17. Proceedings - British Nuclear Energy Soc. Int'l. Conf. on the High Temp. Reactor and Proc. Applic., London, England, November 26-28, 1974.

REACTION EXPERIMENTS FOR THERMOCHEMICAL WATER-SPLITTING

John Gahimer, Jon Pangborn, Stephan Foh,
Mono Mazumder, and Robert Stotz

Institute of Gas Technology
3424 South State Street
Chicago, Illinois 60616

INTRODUCTION

A thermochemical water-splitting process is a sequence of chemical reactions in which every species except water is recycled. Ideally, the net inputs are only water and thermal energy. The net outputs are hydrogen, oxygen, and degraded heat. Thermochemical water-splitting processes offer a closed-cycle, non-material-polluting route to fuel synthesis. They are environmentally compatible because the only by-product is oxygen and because combustion of the product hydrogen re-creates the raw material, water.

In the long term, thermochemical water-splitting processes offer a conversion technology for transforming heat from any moderate- or high-temperature source into chemical energy by using a perpetually available resource. For the near term, hydrogen from a heat source, such as a nuclear reactor, can be used to supplement fossil-fuel sources such as natural gas (blending), petroleum (hydrotreating), and especially coal, shale kerogens, or sand bitumens (hydrogenation to liquids or gases). The American Gas Association is sponsoring a program, now in its fifth year at the Institute of Gas Technology, to theoretically and experimentally evaluate thermochemical water-splitting as a method of fuel production. If hydrogen and oxygen can be produced by a water-splitting process at low cost, they would assume increased importance as industrial commodities as well as fuel sources.

Ideally, water can be split into hydrogen and oxygen by supplying the enthalpy of reaction with a combination of thermal energy (for entropy requirements) and work energy (for free-energy requirements). The present technology for water-splitting is electrolysis, in which work energy (electricity) in excess of the reaction enthalpy is supplied to produce hydrogen and oxygen from a water-electrolyte solution. A heat-to-work transformation is needed to generate the required electrical energy from primary thermal energy (fossil, nuclear, or solar). The efficiency of this transformation is restricted by thermodynamic limitations and by practical constraints in operating power plants. Photolysis processes will encounter a similar restriction if the light is produced from thermal primary energy. Direct solar energy input to photolysis seems limited by the small fraction of the solar spectrum that has sufficient energy, per photon, to drive known photolytic reactions.

To reduce the requirement for a heat-to-work cycle, water can be decomposed in a single step by heating it to very high temperatures (2500° to 4000°C) and separating the gaseous products. The materials required for containment and separation obviously limit practical applications at these temperatures. The same thermal decomposition and separation can be accomplished through multiple chemical reaction steps operating at lower temperatures, i. e., through a thermochemical water-splitting process. According to the second law of thermodynamics, quantities of heat in excess of the reaction free energy plus entropy requirements of water-splitting must be supplied. The chemical reactions are driven primarily by heat inputs, with minimal process work (mechanical and electrical) requirements. Research at IGT has emphasized these processes, for which the predominant form of energy input is heat, with the expectation of more efficient and less capital-intensive processes than those depending primarily upon conversions of heat to work, such as electrolysis.

CLASSES OF KNOWN CYCLES

Nearly all the (pure) thermochemical water-splitting cycles (i. e., closed-loop reaction sequences operated predominantly with thermal energy inputs) published to date (1) can be grouped into one of the five generic classes shown in Table 1.

Table 1. CLASSES OF KNOWN THERMOCHEMICAL HYDROGEN PRODUCTION CYCLES

Class 1: Metal-Metal Oxide Cycles

$M + H_2O \rightarrow MO + H_2$

$MO \rightarrow M + 1/2 O_2$

Class 2: Metal Oxide-Metal Hydroxide Cycles

$M + 2H_2O \rightarrow M(OH)_2 + H_2$

$M(OH)_2 \rightarrow MO + H_2O$

$MO \rightarrow M + 1/2 O_2$

Class 3: Metal Oxide-Metal Sulfate Cycles

$MO + SO_2 + H_2O \rightarrow MSO_4 + H_2$

$MSO_4 \rightarrow MO + SO_3$

$SO_3 \rightarrow SO_2 + 1/2 O_2$

Class 4: Metal-Metal Halide Cycles

$M + 2HX \rightarrow MX_2 + H_2$

$MX_2 \rightarrow M + X_2$

$X_2 + H_2O \rightarrow 2HX + 1/2 O_2$

Class 5: Metal Oxide-Metal Halide Cycles

$M + H_2O \rightarrow MO + H_2$

$MO + 2HX \rightarrow MX_2 + H_2O$

$MX_2 \rightarrow M + X_2$

$X_2 + H_2O \rightarrow 2HX + 1/2 O_2$

(In this table, M can be interpreted as either a zero-valent metal or the lower valance state of an oxide pair or halide pair.) Of course, other types of cycles are possible for hybrid electrothermochemical cycles that include one or more electrolytic steps with work energy (electricity) input. Other types of cycles can also be derived for other forms of work energy input, such as photolysis.

Of course, myriad combinations of these five classes can be made. In general, however, the simpler schemes are expected to be more desirable in terms of both efficiency and capital cost.

No two-step thermochemical cycles, the metal-metal oxide cycles (Class 1 in Table 1) are known to be operable within the temperature range of interest for this program, 300° to 1200°K. Two-step cycles theoretically might be constructed from metal-metal hydride pairs; none have been reported. Many compounds theoretically can form three-step cycles of the metal oxide-metal hydroxide Class 2 or the metal oxide-metal sulfate Class 3. The sulfuric acid cycle investigated by Bowman et al. at Los Alamos Scientific Laboratory (2) and by Brecher et al. at Westinghouse Electric Corp. (3) could be considered a member of both Class 2 with M = sulfur dioxide and of Class 3 with MO = water.

The metal-metal halide Class 4, as written in Table 1, is viable only for chlorides and fluorides because bromine and iodine have unfavorable equilibria in the halogen-steam reaction (the analog of the reverse-Deacon reacton. Because the metal fluorides are relatively stable, cycles involving them are usually not very energy efficient, and fluorine and hydrogen fluoride present obvious containment problems at high temperatures. Thus the chlorides are most practical. Except for rare earth compounds, the only metal-metal chloride pair that we have found to be thermodynamically feasible in three-step cycles of Class 4 (for the 300° to 1200°K temperature envelope available from an HTGR nuclear heat source) is $CrCl_2$-$CrCl_3$.

Some specific examples of chemical reaction sequences for these five generic classes of thermochemical water-splitting cycles are shown in Table 2, along with temperatures at which the reactions should theoretically proceed. Also tabulated are the Gibbs' free-energy change and enthalpy change for each reaction at the stated temperature, and calculated "maximum attainable" energy efficiency for each cycle based on the stated temperature sequence, assuming only near-term technology. "Maximum attainable" energy efficiency is our nomenclature for a figure of merit which is the upper limit of the process flowsheet efficiency calculation. Our efficiency calculation methodology has been discussed in previous papers (4, 20).

Several methods of calculating cycle efficiencies have been proposed (9-13). The IGT method assumes that all primary input energy is heat and that the product energy is the high heating value of the hydrogen produced. It is based on an energy and material balance for the cycle, and it takes into account the work terms due to poor reaction yields and reactant recycles, gas separations, electrochemical steps, and compressions, with a credit for work generated from excess heat available at greater than 600°K. Heat exchange within the cycle is optimized by inspection. Thermodynamic quantities are taken or calculated from standard reference works on the thermodynamic properties of materials (5-8). A computer program utilizing essentially the same methodology has been developed by the University of Kentucky (11). (This program gives somewhat lower values for cycle efficiency than does IGT's calculation because of differences in the pattern of internal heat transfer and assumptions about the efficiency of generating work from heat.)

The example cycles shown in Table 2 are in the high end of the efficiency range we have found for feasible thermochemical cycles, with "maximum attainable" efficiencies ranging from 47% to 65%. They illustrate the general trend that cycles with few steps and high input temperatures have higher efficiencies, as expected, and that thermodynamically feasible and efficient cycles, for the 300° to 1500°K temperature span, usually have individual reaction steps whose Gibbs' free-energy change is in the range of about −15 to about +15 kilocalories.

Table 2. EXAMPLES OF KNOWN THERMOCHEMICAL HYDROGEN PRODUCTION CYCLES

	Temp, °K	G^o_T, kcal	H^o_T, kcal
Metal-Metal Oxide Cycle L-1 (65% "Maximum Attainable" Efficiency)			
$Cd(s) + H_2O(g) \rightarrow CdO(s) + H_2(g)$	400	+1.8	−3.1
$CdO(s) \rightarrow Cd(g) + 1/2\,O_2(g)$	1500	+8.7	+84.8
Metal Oxide-Metal Hydroxide Cycle L-2 (65% "Maximum Attainable" Efficiency)			
$Cd(s) + 2H_2O(\ell) \rightarrow Cd(OH)_2(s) + H_2(g)$	Electrolysis	+1.0	+3.4
$Cd(OH)_2(s) \rightarrow CdO(s) + H_2O(g)$	650	0.0	+12.3
$CdO(s) \rightarrow Cd(g) + 1/2\,O_2(g)$	1500	+8.7	+84.8
Metal Oxide-Metal Sulfate Cycle C-7 (57% "Maximum Attainable" Efficiency)			
$Fe_2O_3(s) + 2SO_2(g) + H_2O(g) \rightarrow 2FeSO_4(s) + H_2(g)$	400	−8.8	−46.6
$2FeSO_4(s) \rightarrow Fe_2O_3(s) + SO_2(g) + SO_3(g)$	1000	−0.9	+78.8
$SO_3(g) \rightarrow SO_2(g) + 1/2\,O_2(g)$	1200	−3.3	+23.1
Metal-Metal Halide Cycle J-1 (47% "Maximum Attainable" Efficiency)			
$2CrCl_2(s) + 2HCl(g) \rightarrow 2CrCl_3(s) + H_2(g)$	600	0.0	−30.8
$2CrCl_3(s) \rightarrow 2CrCl_2(\ell) + Cl_2(g)$	1200	+15.1	+86.5
$Cl_2(g) + H_2O(g) \rightarrow 2HCl(g) + 1/2\,O_2(g)$	1200	−5.4	+14.2
Metal Oxide-Metal Halide Cycle B-1 (47% "Maximum Attainable" Efficiency)			
$3FeCl_2(\ell) + 4H_2O(g) \rightarrow Fe_3O_4(s) + 6HCl(g) + H_2(g)$	1200	−0.3	+45.8
$Fe_3O_4(s) + 8HCl(g) \rightarrow 2FeCl_3(s) + FeCl_2(s) + 4H_2O(g)$	400	−13.4	−58.8
$2FeCl_3(s,g) \rightarrow 2FeCl_2(s) + Cl_2(g)$	700	−5.7	−37.8
$Cl_2(g) + H_2O(g) \rightarrow 2HCl(g) + 1/2\,O_2(g)$	1200	−5.4	+14.2

From the examples in Table 2, we can also conclude that thermochemical water-splitting is potentially a very efficient technology for transforming primary heat energy into secondary fuel energy. IGT has theoretically examined about 150 specific examples of such cycles. Of these, about 90 are thermodynamically feasible and about 60 meet our criteria for warranting some experimental work ("maximum attainable" efficiency greater than 35% and no compounds of unmanageable corrosivity).

EXPERIMENTAL OBJECTIVE AND PROCEDURES

The experimental objective is to determine which cycles are technically feasible and whether their efficiency is still attractive at actual operating conditions. Thus, our experimental program examines the reaction steps of theoretically possible and potentially efficient cycles to identify those that are truly workable. Undocumented reaction steps are tested in the laboratory to determine feasibility, practicality, and yields at operating conditions. Documented reaction steps are verified, including operating conditions different from those reported in the literature, and the morphology of solid products is determined.

Our purpose is to prove the feasibility of performing certain chemical reactions by supplying primarily heat energy. Reactions that require excessive work energy are undesirable; therefore, we usually construct uncomplicated reaction systems that do not involve mixing or fluidization. In the preliminary reaction trials reported here, total pressure is always about 1 atmosphere.

Our standard procedure is to expose 5 to 50 grams of solid or liquid reactant, in an inert ceramic boat or in a packed bed, to a continuous flow of gaseous reactant or inert carrier gas. The systems are operated as batch reactors (for solid materials) with gaseous product removal. All materials exposed to the reaction are glass, quartz, or ceramic. When a 25% or more conversion (mole basis) occurs in 1 to 2 hours with reagent-grade reactants, we consider that reaction to be proved "workable." When all the reactions of a cycle are proved workable with reagent-grade materials, and we have operated the entire cycle, step by step, with recycled materials, we consider that cycle to be "demonstrated."

THE GROUP OF IRON-CHLORINE-HYDROGEN-OXYGEN CYCLES

Of the 150 cycles that we have theoretically examined, only 12 are experimentally workable with reagent-grade materials, and only four of these have been demonstrated with recycled materials. To our knowledge, another five cycles have been shown to be experimentally workable by other research groups, and we understand that one of these has been demonstrated (19). Interestingly, of this total of 17 known workable cycles, 12 belong to the group of metal oxide-metal halide cycles (Class 5 in Table 1) that are constructed from the elements iron-chlorine-hydrogen-oxygen. The nine chemical reactions shown in Table 3 are sufficient to construct five of these 12 cycles. The other seven known cycles of this group involve substituting two reactions for one of those listed or combining two reactions into one.

The following discussion of our experimental results is organized into four functional sections: metal oxidation (Reactions 1 and 2), metal halogenation (Reactions 3, 4, and 5), metal reduction (Reactions 6 and 7), and halogen recycle (Reactions 8 and 9).

Table 3. REACTIONS OF THE IRON-CHLORINE-HYDROGEN-OXYGEN GROUP OF CYCLES

No.		T, °K	ΔG_T^0, kcal	ΔH_T^0, kcal	Cycles
	Metal Oxidation				
1	$3Fe(s) + 4H_2O(g) \rightarrow Fe_3O_4(s) + 4H_2(g)$	800	− 9.3	−26.7	A-1, A-2
2	$3FeCl_2(s) + 4H_2O(g) \rightarrow Fe_3O_4(s) + 6HCl(g) + H_2(g)$	1200	− 0.3	+45.8	B-1, B-2, I-6
	Metal Halogenation				
3	$Fe_3O_4(s) + 8HCl(g) \rightarrow 2FeCl_3(s) + FeCl_2(s) + 4H_2O(g)$	400	−13.4	−58.8	A-1, B-1
4	$Fe_3O_4(s) + 9/2\,Cl_2(g) \rightarrow 3FeCl_3(g) + 2O_2(g)$	1200	+11.1	+ 73.0	A-2, B-2
5.	$Fe_3O_4(s) + 3/2\,Cl_2(g) + 6HCl(g) \rightarrow 3FeCl_3(s) + 3H_2O(g) + 1/2\,O_2(g)$	400	−11.4	− 65.3	I-6
	Metal Reduction				
6	$2FeCl_3(s) \rightarrow 2FeCl_2(s) + Cl_2(g)$	700	−5.7	− 37.8	A-1, A-2, B-1, B-2, I-6
7	$3FeCl_2(\ell) + 3H_2(g) \rightarrow 3Fe(s) + 6HCl(g)$	1200	+ 1.4	+ 71.3	A-1, A-2
	Halogen Recycle				
8	$Cl_2(g) + H_2O(g) \rightarrow 2HCl(g) + 1/2\,O_2(g)$	1200	−5.4	− 14.2	A-1, B-1
9	$6HCl(g) + 3/2\,O_2(g) \rightarrow 3Cl_2(g) + 3H_2O(g)$	400	−22.5	− 41.3	A-2, B-2

METAL OXIDATION

Reactions 1 and 2 are the hydrogen-producing steps of these cycles, i.e., the reduction of steam to molecular hydrogen by using steam to oxidize a metal or metal halide species. We would theoretically prefer to make Fe_2O_3 in either reaction, since it would produce more hydrogen per unit of solid, but the more stable Fe_3O_4 predominates. The Fe_2O_3 probably offers only a theoretical, not a real, advantage because the kinetics of the subsequent halogenation reaction are slower with Fe_2O_3 than with Fe_3O_4.

1) $$3Fe + 4H_2O \rightarrow Fe_3O_4 + 4H_2$$

The steam-iron reaction is well-known industrial technology. A modern, continuous version of it is the hydrogen-producing step in one variation of IGT's HYGAS Process for the synthesis of pipeline gas from coal (15-17). The free-energy change for this reaction is favorable over the entire temperature span of interest, as shown in Figure 1. Our experimental tests found a minimum useful temperature of 600°C, where 44% conversion was obtained. Greater conversions can be obtained at higher temperatures because of improved reaction kinetics. The reaction conversion also depends on iron morphology.

2) $$3FeCl_2 + 4H_2O \rightarrow Fe_3O_4 + 6HCl + H_2$$

For the steam-$FeCl_2$ reaction, free-energy changes (Figure 1) are negative only above 920°C. However, the reaction proceeds to some extent at 400°C, with excess steam flow and continuous removal of HCl and hydrogen; the solid product is a mixture of Fe_3O_4, Fe_2O_3, and FeOCl. At higher temperatures, higher yields of Fe_3O_4 and higher total conversions are noted. Essentially complete conversion to oxides occurs in less than 2 hours at 600°C (again, with excess steam flow). No undesired side reactions are observed, but significant quantities of FeOCl are produced, particularly at temperatures below 600°C, if the reaction is stopped short of completion. Apparently the oxychloride is an intermediate product; it vanishes if reacted further with steam at the higher temperatures.

The Appendix details a new method of analysis that we have developed for the iron oxides.

METAL HALOGENATION

Reactions 3 and 4 are metal halogenation, the reaction of metal oxide with halogen or halogen acid to produce metal halide. A simple substitution of chloride for oxide occurs in Reaction 3; in Reaction 4, one of the three iron atoms is oxidized. Reaction 5 is a combination of halogenation and halogen recycle; it performs the functions of both Reaction 4 and Reaction 9. These reactions, particularly 4 and 5, can also be viewed as the oxygen release reactions.

3) $$Fe_3O_4 + 8HCl \rightarrow 2FeCl_3 + FeCl_2 + 4H_2O$$

Based on the free-energy change for Reaction 3 (Figure 2), reasonable reaction yields are expected and observed at temperatures below 250°C. In a vertical, packed-bed reactor with slight excess HCl flow, Reaction 3 proceeds to complete conversion in 2 to 5 hours over the entire temperature span 200° to 400°C. Stoichiometry of the condensed products agrees with stoichiometry of Reaction 3, indicating that the $FeCl_3$ decomposition, Reaction 6, does not proceed concurrently at this temperature when excess HCl is present.

The gases evolved from the reaction are HCl, excess H_2O, and the dimer, Fe_2Cl_6. Small quantities of FeOCl also are present, depending on operating conditions. If the Fe_2Cl_6 is allowed to solidify in the presence of condensing steam, a hydrate is formed. Dehydration of the $FeCl_3$ hydrate is difficult and usually results in the formation of Fe_2O_3, which is not desirable at this step in the cycles. Because of this, we normally operate this reactor with an exit zone where the temperature is only slightly greater than 100°C, and the Fe_2Cl_6 solidifies in this zone.

4) $$Fe_3O_4 + 9/2\,Cl_2 \rightarrow 3FeCl_3 + 2O_2$$

The free-energy change of Reaction 4 (Figure 2) decreases continuously with increasing temperature. Although the equilibrium is quite unfavorable above 725°C, the reaction does proceed significantly at these temperatures with excess chlorine flow and continuous removal of the gaseous Fe_2Cl_6 and oxygen products. Conversions of 26% in 2 hours were observed at temperatures as low as 800°C. Complete conversion was obtained in 5 hours at 925°C. Chlorine gas, being a stronger oxidizing agent than HCl, produces only $FeCl_3$ as an iron-containing product, whereas in Reaction 3, both $FeCl_3$ and $FeCl_2$ are produced. Concurrent decomposition of $FeCl_3$ occurs neither in the presence of chlorine for Reaction 4, at these temperatures, nor in the presence of HCl for Reaction 3.

5) $$Fe_3O_4 + 3/2\,Cl_2 + 6HCl \rightarrow 3FeCl_3 + 3H_2O + 1/2\,O_2$$

Figure 2 shows that Reaction 5 is thermodynamically favored at temperatures below 225°C. We find essentially complete conversion from 125° to 200°C in a packed-bed reactor with downflow of excess gaseous reactants and continuous removal of gaseous products. The product analyses do not match the reaction stoichiometry as written. For instance, in the trial at 150°C, the product solids were 80 mole % $FeCl_3$ and 20 mole % FeOCl.

In these experiments the reactant gases, chlorine and HCl, in the correct stoichiometric ratio are metered into the reaction zone together. The reaction zone contains a moderate vapor pressure of the gaseous dimer, Fe_2Cl_6, from the $FeCl_3$ reaction product, and some of this dimer passes downward through the packed bed along with the other gaseous reaction products. Below the solid bed, an exit temperature zone of slightly above 100°C is maintained to solidify the Fe_2Cl_6 without allowing steam condensation; however, we always find FeOCl in the solid product below the bed. Experimental configurations without the intermediate temperature zone produce more FeOCl. By removing the FeOCl and further treating it with HCl or chlorine gas, the FeOCl can be converted to $FeCl_3$, maintaining a closed cycle.

METAL REDUCTION

Reactions 6 and 7 are halide decomposition and the reaction of halide with hydrogen to produce metal. They reduce the metal atom oxidation state, and they are the most difficult steps to operate experimentally. This difficulty is not surprising because the product of these reactions must be capable of reducing water to molecular hydrogen. As shown in Figure 3, Reaction 7 is thermodynamically favored only at temperatures above about 950°C, and Reaction 6 is favored only in a narrow temperature range (700° to 800°K). Even this is an oversimplification for Reaction 6, because the competing reaction of $FeCl_3$ to gaseous dimer is significant at these temperatures.

6) $$2FeCl_3(s) \rightarrow 2FeCl_2(s) + Cl_2(g)$$

Because of the competing favorable equilibrium of $FeCl_3$ to the relatively more stable gaseous dimer Fe_2Cl_6 and the quite unfavorable equilibrium of the dimer-to-$FeCl_2$ reaction, Reaction 6 exhibits poor yields when operated by normal techniques. The dimer is present over the entire temperature range of interest. Although $FeCl_3$ has a boiling point of 332°C and a melting point of 302°C, we have observed formation of the gaseous dimer (by sublimation) at temperatures as low as 225°C. In a horizontal reactor with inert gas flow, the conversion to $FeCl_2$ is less than 5%. In a system with no external flow, purged initially with inert gas and with a cooled exit open to atmospheric pressure, we find slightly improved conversions of 9.5% down to 2.1% over the temperature span 225° to 500°C. By repeated cycling of material, the best overall yield is about 20% in 5 hours.

Reaction 6 can be replaced by a pair of reactions that perform the same function:

$$FeCl_3 + CuCl \rightarrow FeCl_2 + CuCl_2$$

$$CuCl_2 \rightarrow CuCl + 1/2Cl_2$$

The first reaction is performed by placing a layer of CuCl in stoichiometric excess on top of a layer of $FeCl_3$. As expected from reaction free-energy change calculations, the reaction proceeds at temperatures below 290°C. Complete conversion is obtained at 280°C in 2 hours. Only slight traces of $FeCl_3$ escape the CuCl layer.

The second reaction is more complicated, because $FeCl_2$ and $CuCl_2$ cannot be easily separated. The reaction is thermodynamically favored above 500°C, but when the mixture from the first reaction is heated to this temperature the products are $FeCl_3$ and CuCl. Temperature staging allows the decomposition of $CuCl_2$ to proceed with minimum concurrent reoxidation of the $FeCl_2$. At temperatures of 275° to 325°C, the following reaction occurs:

$$10FeCl_2 + 10CuCl_2 \rightarrow 7FeCl_3 + 3FeCl_2 + 10CuCl + 3/2Cl_2$$

After chlorine has been swept from the reaction zone, the products can be reduced in temperature and the first reaction repeated to yield:

$$7FeCl_3 + 3FeCl_2 + 10CuCl \rightarrow 10FeCl_2 + 7CuCl_2 + 3CuCl$$

If these two reactions are cycled repeatedly with chlorine removal, the end products are $FeCl_2$ and CuCl. CuCl is insoluble in water, whereas $FeCl_2$ is soluble. If necessary, the mixture of these two components can be separated by this means, and each can be recycled to its use point.

Although the CuCl reaction scheme does provide essentially complete conversion of $FeCl_3$ to $FeCl_2$, the replacement of one reaction by these two staged reactions is not desirable because it involves additional energy consumption.

7) $$FeCl_2 + H_2 \rightarrow Fe + 2HCl$$

Figure 3 shows that the free-energy change for Reaction 7 decreases with increasing temperature, but is still slightly positive even at 925°C. The reaction does proceed, however, at 800° to 925°C with excess hydrogen flow. We find 90% conversion in 2 hours at 800°C; the other 10% of the $FeCl_2$ does not react only because it sublimes from the reaction zone to a colder section of the reactor.

HALOGEN RECYCLE

Reactions 8 and 9 are the reduction of halogen or the oxidation of halogen acid. The reverse-Deacon and Deacon reactions are the method for recycling halogen or halogen acid and thereby closing each cycle. The reverse-Deacon (Reaction 8) is particularly important in thermochemical hydrogen production cycles; it is the oxygen-liberating step in 17 of the cycles we have examined experimentally. As Figure 4 illustrates, the reverse-Deacon reaction is favored above 590°C, and the Deacon reaction is favored below this temperature.

8) $$Cl_2 + H_2O \rightarrow 2HCl + 1/2O_2$$

Because the reverse-Deacon reaction is completely homogeneous, a simple, heated ceramic tube with cooled exit line was utilized as the reactor. For a mixture of chlorine with excess steam, conversion, based on chlorine, varied from 92% to 98% for the temperature range 700° to 900°C. Apparently the reaction attains near-equilibrium conversions at these temperatures, even without a catalyst. As illustrated by the reaction free-energy changes (Figure 4), the equilibria are quite favorable. Thus, only a slight excess of steam is needed for complete conversion.

9) $$2HCl + 1/2O_2 \rightarrow Cl_2 + H_2O$$

The Deacon reaction is a well-known industrial process(18) and its equilibrium and reaction-rate data are well documented. We verified operation at a temperature of 200°C without a catalyst, which parallels the operating conditions of the industrial processes with catalysts. A stoichiometric mixture of HCl and oxygen, passed through a reaction tube identical to that described above, was completely converted in 1 minute of residence time.

EFFICIENCY OF THE IRON-CHLORINE-HYDROGEN-OXYGEN GROUP OF CYCLES

From the nine reactions discussed above, we can construct five cycles that typify the iron-chlorine-hydrogen-oxygen group. In the IGT nomenclature system, these five cycles are denoted as A-1, A-2, B-1, B-2, and I-6. Table 4 lists the reaction steps (of Table 3) that constitute each cycle and the calculated "maximum attainable" efficiencies, assuming the reaction temperatures of Table 3.

Table 4. TYPICAL SET OF THE IRON-CHLORINE-HYDROGEN-OXYGEN GROUP OF CYCLES

IGT Cycle	Reaction Steps	"Maximum Attainable" Efficiency, %
A-1	1, 3, 6, 7, 8	40
A-2	1, 4, 6 (X 1.5), 7, 9	30
B-1	2, 3, 6, 8	47
B-2	2, 4, 6 (X 1.5), 9	35
I-6	3, 5, 6 (X 1.5)	47

Cycle B-1 has been independently derived by Abraham and Shreiner of Argonne National Laboratory (10), although they apparently have done no experimental work with it. Cycle I-6 is our designation for EURATOM's Mark-9 cycle (14), derived by Hardy of the EURATOM laboratory in Ispra, Italy; it is currently the subject of continued work by that laboratory. Cycles B-1 and I-6 also have the highest "maximum attainable" efficiency of this group at 47%.

Using the experimentally determined conditions of operability for individual reactions, we can calculate a more realistic value of "maximum attainable" efficiency for these cycles. Because the intention of the experiments reported here is simply to determine reaction feasibility to differentiate workable from nonworkable cycles, mass-transfer and reaction rates have temporarily been given only secondary importance. Our reactor design, mass-transfer rate, and reactant surface area could be much improved for any specific reaction, and this would greatly enhance the observed kinetics and yields.

We have recalculated the "maximum attainable" efficiency for cycles B-1 and I-6 with reaction temperatures at known experimental operating conditions. This efficiency drops to about 43% for both cycles, versus the 47% calculated by assuming the thermodynamic optimum temperature conditions listed in Table 3.

CONCLUSIONS

Almost all known pure thermochemical hydrogen production cycles can be grouped into five generic classes, each involving either a metal oxide or a metal halide as an intermediate.

In general, those cycles with the highest-temperature endothermic reactions and the least number of reactions are the most efficient. This is expected because thermochemical cycles are special types of heat engines. The "maximum attainable" efficiency of known published cycles is about 65% with 1225°C input heat and assuming present technology for conversion of heat to work.

The most difficult step in any thermochemical cycle is usually the one involving a change in metal oxidation state, usually the reduction. It is often necessary to operate such a step with some work input, such as electrolysis. Because of this, few of the truly efficient and workable hydrogen production cycles are purely thermochemical.

Of those thermochemical hydrogen production cycles that are known to be workable with reagent-grade materials, more than two-thirds are of the group constructed from compounds of iron, chlorine, hydrogen, and oxygen. The "maximum attainable" efficiency for cycles of this group is about 47% with 925°C input heat and present technology for conversion of heat to work. This efficiency drops to about 43% if the reaction steps are assumed to operate at temperatures of proven workability rather than at theoretically optimum temperatures based on thermodynamics.

ACKNOWLEDGMENT

The author is indebted to John Sharer for his many technical contributions to this research program.

This research is part of Project IU-4-14,"Thermochemical Hydrogen Production," sponsored by the American Gas Association; Dr. A. Flowers of A.G.A. is the program manager. We gratefully acknowledge the continued support of the A.G.A. for development of this technology.

REFERENCES

1. Sharer, J. and Pangborn, J., "Survey of Programs on Thermochemical Hydrogen Production," Chapter 6 in Gillis, J. et al., Survey of Hydrogen Production and Utilization Methods, Vol. II of Institute of Gas Technology Report to NASA Marshall Space Flight Center, Huntsville, Ala., Contract No. NAS 8-30757, August 1975.

2. Bowman, M. G. et al., "Hydrogen Production by Low Voltage Electrolysis in Combined Thermochemical and Electrochemical Cycles." Paper presented at the 146th Meeting of the Electrochemical Society, New York, October 1974.

3. Brecher, L. E. et al., "Studies of the Use of Heat From High Temperature Nuclear Sources for Hydrogen Production Processes," NASA Lewis Research Center Report CR-134918, Tasks 1 and 2.

4. Pangborn, J. and Sharer, J., "Analysis of Thermochemical Water-Splitting Cycles,"in Veziroglu, T.N. Ed., Hydrogen Energy, 499-515. New York: Plenum Press, 1975.

5. Stull, D. R. and Prophet, H., JANEF Thermochemical Tables, 2nd Ed., NBS Publication No. NSRDS-NBS 37. U.S. Department of Commerce, June 1971.

6. Rossini, F. D. et al., Selected Values of Chemical Thermodynamic Properties, NBS Circular 500. U.S. Department of Commerce, February 1952.

7. Coughlin, J. P., Heats and Free Energies of Formation of Inorganic Oxides, Bureau of Mines Bulletin 542. Washington, D. C.: U.S. Department of Interior 1954 .

8. Wicks, C. E. and Block, F. E., Thermodynamic Properties of 65 Elements — Their Oxides, Halides, Carbides, and Nitrides, U.S. Bureau of Mines Bulletin 605. Washington, D. C.: U.S. Department of Interior 1963 .

9. Funk, J., "Thermodynamics of Multi-Step Water Decomposition Processes," Am. Chem. Soc. Div. Fuel Chem. 16, No. 4, 49-87 (1972).

10. Abraham, B. and Schreiner, F., "General Principles Underlying Chemical Cycles Which Thermally Decompose Water into the Elements," Ind. Eng. Chem. Fundam. 13, No. 4, 305-310 (1974).

11. Funk, J., Conger, W. and Carty, R., "Evaluation of Multi-Step Thermochemical Processes for the Production of Hydrogen From Water," in Veziroglu, T. N., Ed., Hydrogen Energy, 457-470. New York: Plenum Press, 1975.

12. Chao, R., "Thermochemical Water Decomposition Processes," Ind. Eng. Chem. 13, 94-101 (1974).

13. Fueki, K., "Application of Free Energy Diagrams to Thermochemical Processes," University of Tokyo, Japan, 1975.

14. DeBeni, G. et al., "Thermochemical Water-Splitting as a Method for Hydrogen Production." Paper III-17 of British Nuclear Engineering Society Meeting, London, November 1974.

15. Tarman, P. B., "Status of the Steam-Iron Program." Paper presented at 7th Synthetic Pipeline Gas Symposium, Institute of Gas Technology, Chicago, October 1975.

16. Institute of Gas Technology, Process Research Division, "HYGAS — 1972 to 1974," IGT Report 110, ERDA Report FE-1221-1. Washington, D. C.: U.S. Energy Research and Development Administration, July 1975.

17. Institute of Gas Technology, "Development of the Steam-Iron System for Production of Hydrogen for the HYGAS Process," Interim Report 1, OCR Contract No. 14-32-0001-1518, Chicago, August 1974.

18. Furusaki, S., "Catalytic Oxidation of Hydrogen Chloride in a Fluid Bed Reactor," AIChE J. 19, 1009-1016 (1973) September.

19. Bowman, M. G., "Thermochemical Production of Hydrogen From Water," Quarterly Report LA-5731-PR. Los Alamos, N. M., Los Alamos Scientific Laboratories, June 1974.

20. Pangborn, J. B., "Laboratory Investigations on Thermochemical Hydrogen Production." Paper presented at The First World Hydrogen Energy Conference, Miami Beach, March 1976.

Appendix. ANALYSIS OF Fe_2O_3/Fe_3O_4 MIXTURES

Because Fe_3O_4 contains 1 mole of Fe^{+2} per mole of oxide, the concentration of this oxide can be determined by measuring the concentration of Fe^{+2}. To dissolve a mixture of the oxides Fe_2O_3 and Fe_3O_4, a strong acid is required; unfortunately, Fe^{+2} is readily oxidized in a strongly acid solution. This problem can be circumvented by placing a known amount of a standard oxidizing agent, $K_2Cr_2O_7$, in the acidic solvent. As the oxides dissolve, the Fe^{+2} is quantitatively oxidized in situ. Thus, the concentration of Fe^{+2} can be determined indirectly by a back titration with a standard Fe^{+2} solution to measure the unreacted portion of the standard oxidizing agent.

The concentration of Fe_2O_3 in the sample is determined indirectly by measuring the total iron concentration via a potassium dichromate titration. After the quantity of iron present as Fe_3O_4 has been subtracted (this would be 3 times the Fe^{+2} concentration), the concentration of Fe_2O_3 can be calculated.

The above procedure can also be applied with slight modification to Cu_2O/CuO mixtures. The determination of Cu^+ is identical to the procedure for Fe^{+2}. The total copper concentration, however, is determined by an EDTA titration.

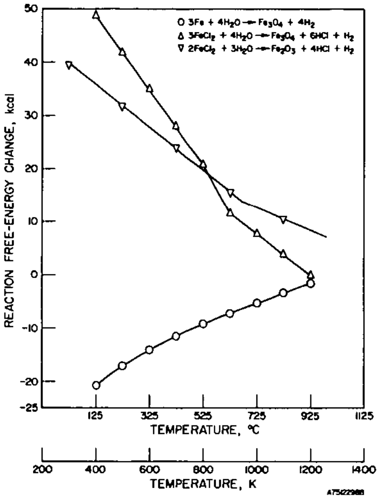

Figure 1. FREE-ENERGY CHANGE FOR THE METAL OXIDATION REACTIONS

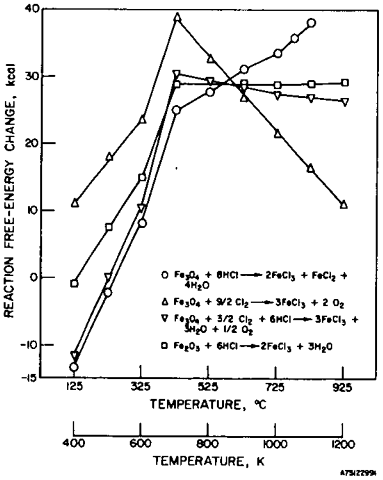

Figure 2. FREE-ENERGY CHANGE FOR THE METAL HALOGENATION REACTIONS

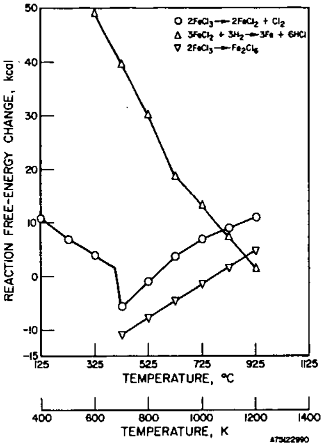

Figure 3. FREE-ENERGY CHANGE FOR THE METAL REDUCTION REACTIONS

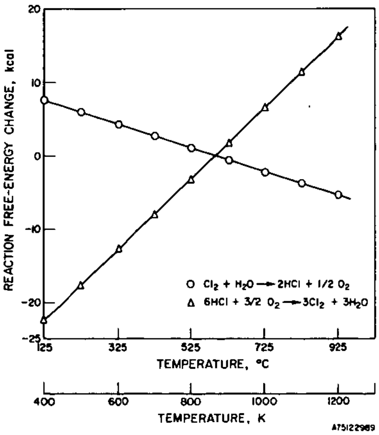

Figure 4. FREE-ENERGY CHANGE FOR THE HALOGEN RECYCLE REACTIONS

THERMOCHEMICAL DECOMPOSITION OF WATER BASED ON REACTIONS OF CHROMIUM AND STRONTIUM COMPOUNDS*

C. E. Bamberger and D. M. Richardson

CHEMISTRY DIVISION, OAK RIDGE NATIONAL LABORATORY, Oak Ridge, TN 37830

The predictable future shortage of natural gas as a raw material for the production of hydrogen will require the use of water, an inexhaustible source. High efficiency decomposition of water may be attained by thermochemical cycles in which energy is expended primarily as heat. Although over seventy thermochemical cycles have been proposed(1) only a small fraction appears to merit further consideration. Continued research and investion will asure that the most efficient and practical cycles are developed. The chemistry of ternary oxides of chromium makes possible a closed cycle consisting of three reactions. One such cycle involving barium chromates (IV), (V) and (VI) has been described(2). This paper reports a similar cycle of the strontium chromates (IV), (V) and (VI) that affords lower temperatures and easier separations than prevail in the barium cycle.

The proposed cycle consists of the following reactions:

$$Cr_2O_3(s) + 4SrO(s) + H_2O(g) \xrightarrow{\sim 1000K} 2Sr_2CrO_4\ (s) + H_2(g) \qquad (1)$$

$$2SrCrO_4(s) + 4/3Sr(OH)_2(\ell) \xrightarrow{\sim 800K} 2/3Sr_5(CrO_4)_3OH(s) + H_2O(g) + 1/2O_2(g) \qquad (2)$$

$$2Sr_2CrO_4(s) + 2/3Sr_5(CrO_4)_3OH(s) + 5H_2O(\ell) \xrightarrow{\sim 400K,\ \text{aqueous}}$$

$$Cr_2O_3(s) + 2SrCrO_4(d) + 16/3Sr(OH)_2(d) \qquad (3)$$

where (d), (g), (ℓ) and (s) refer, respectively, to the states dissolved, gaseous, liquid and solid. The net reaction is H_2O decomposing to H_2 and $1/2O_2$.

These reactions were experimentally confirmed in laboratory equipment at one atmosphere total pressure under flowing argon. According to published results(3) Cr_2O_3 is not oxidized by $Sr(OH)_2$. Our work, however, showed partial reaction with 28% of expected hydrogen being evolved. Starting from ambient the temperature was continuously increased and maximum hydrogen pressure was observed at 800°C followed by rapid decline. This was to be expected since the dissociation pressure of H_2O over $Sr(OH)_2$ reaches 710 torr at 700°C (4). The addition of LiOH as a flux and additional oxidant (hydroxyl ion) raised the hydrogen yield to 43%. Such additions, however, increase the corrosivity of the mixture and later separation problems would complicate the cycle. It was then demonstrated that the extent of reaction was dependent on the partial pressure of steam and independent of the ratio Sr/Cr. With steam pressure limited to approximately one atmosphere by the equipment used the maximum rate of hydrogen evolution occurred in the

*Research sponsored by the U. S. Energy Research and Development Adminstration under contract with Union Carbide Corportion.

By acceptance of this article, the publisher or recipient acknowledges the U.S. Government's right to retain a non-exclusive, royalty-free license in and to any copyright covering the article.

vicinity of 700°C and 100% yield was obtained below 800°C. The product Sr_2CrO_4 was confirmed by chemical analysis and x-ray powder diffraction.

Reaction (2) was first established by Scholder and Suchy (5) who used a flowing atmosphere of moist nitrogen at 700-1000°C. They also found that the product, $Sr_5(CrO_4)_3OH$, was stable in dry nitrogen up to 850°C. In the present work it was found that a moist purge was not required because the reaction occurs at much lower temperatures, 480-580°C, at which the dissociation pressure of H_2O over $Sr(OH)_2$ is not very large, ≤100 torr(4). The reaction proceeded to completion with only a small excess of Sr $(OH)_2$ over the required stoichiometric ratio; this was confirmed by measurement of O_2 evolved, by chemical analysis and by x-ray diffraction.

Difinitive information was not available on the hydrolytic behavior of Sr_2CrO_4 and of $Sr_5(CrO_4)_3OH$. The former was reported less stable toward water than its barium analog(3,6). In relation to $Sr_5(CrO_4)_3OH$ it was reported that $Ca_5(CrO_4)_3OH$ is not stable in cold water (7) and that $Ba_5(CrO_4)_3OH$ undergoes hydrolytic disproportionation in hot water (2). Experimental determination of the hydrolysis of each compound was conducted in a Soxhlet extractor under argon. The results obtained are represented by the following reactions:

$$2Sr_2CrO_4(s) + 10/3H_2O(\ell) \xrightarrow{\text{aqueous}} 2/3Cr_2O_3(s) + 2/3SrCrO_4(d) + 10/3Sr(OH)_2(d) \quad (3a)$$

$$2/3Sr_5(CrO_4)_3OH(s) + 5/3H_2O(\ell) \xrightarrow{\text{aqueous}} 1/3Cr_2O_3(s) + 4/3SrCrO_4(d) + 2Sr(OH)_2(d) \quad (3b)$$

Since the same hydrolysis products are obtained both reactions can be combined as reaction (3).

The demonstration of reactions (1), (2) and (3) validates the cycle proposed in Fig. 1. The temperatures required have already been exceeded in High Temperature Gas (Cooled) Reactors, the number of reactions is the minimum required (8), and there are no difficult gas separation problems. The laboratory experiments were conducted with static reagents, thus on a dynamic engineering scale it may be expected that kinetics would be more favorable and that lower temperatures would be required. In comparing the Ba-Cr cycle described earlier (2) with the present Sr-Cr one, it is evident that the latter is more attractive on the basis of fewer separation problems and lower reaction temperatures. Although the solubility of $SrCrO_4$ is low, 4.47 mM/ℓ at 25°C, it is about 400 times more soluble than $BaCrO_4$ (9); thus, we were able to separate $SrCrO_4$ completely from Cr_2O_3. The subsequent separation of $SrCrO_4$ and $Sr(OH)_2$ can be easily achieved because of their very different solubilities enhanced by the presence of the common ion Sr^{2+}.

Acknowledgements: We thank K. Cheng, Summer Participant 1974, presently at Brandeis University for his assistance with the experimental work and M. A. Bredig, consultant to the Chemistry Division, ORNL for his interpretation of the x-ray powder diffraction films.

References

1. C. E. Bamberger and D. M. Richardson, Cryogenics, (in print).
2. C. E. Bamberger, D. M. Richardson, M. A. Bredig and K. Cheng, Science, 189, 715 (1975).
3. R. Scholder and G. Sperka, Z. Anorg. Allgem. Chem., 285, 49 (1956).
4. Gmelins Handbuch der Anorganischen Chemie, System #29, p. 161, 8th edn., Verlag Chemie, Weinheim (1960).
5. R. Scholder and H. Suchy, Z. Anorg. Allgem. Chem., 308, 295 (1961).
6. K. A. Wilhelmi Arkiv för Kemi, 26, 157 (1966).
7. R. Scholder and H. Schwarz, Z. Anorg. Allgem. Chem., 326, 11 (1963).
8. B. M. Abraham and F. Schreiner, "General Principles Underlying Chemical Cycles Which Thermally Decompose Water into the Elements", Ind. Eng. Chem. Fundam., 13 (4) (1974), p. 305 .
9. W. F. Linke, Solubilities, Inorganic and Metal Organic Compounds, Vol. I (1958) and II (1965) 4th edn., American Chemical Society, Washington.

ORNL-DWG. 75-17668

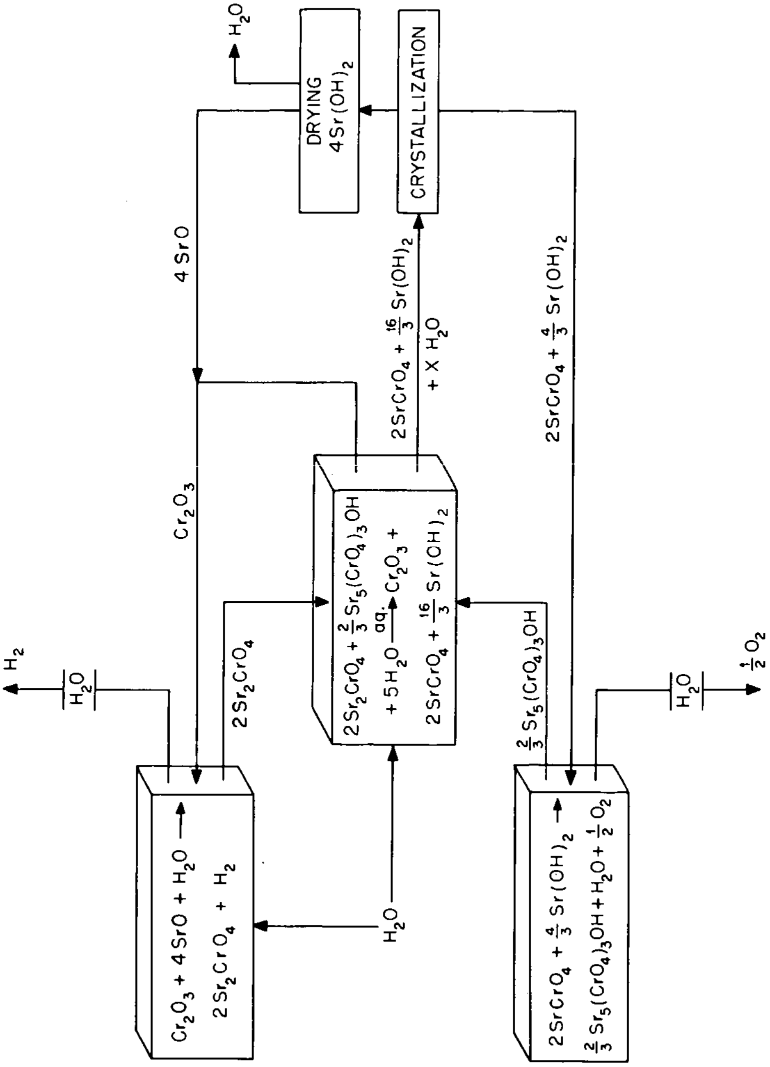
$Cr_2O_3 + 4SrO + H_2O \longrightarrow 2Sr_2CrO_4 + H_2$
H_2
H_2O
$2Sr_2CrO_4$
Cr_2O_3
$4SrO$
H_2O
DRYING $4Sr(OH)_2$
CRYSTALLIZATION
$2Sr_2CrO_4 + \frac{2}{3}Sr_5(CrO_4)_3OH + 5H_2O \xrightarrow{aq.} Cr_2O_3 + 2SrCrO_4 + \frac{16}{3}Sr(OH)_2$
$2SrCrO_4 + \frac{16}{3}Sr(OH)_2 + X H_2O$
H_2O
$\frac{2}{3}Sr_5(CrO_4)_3OH$
$2SrCrO_4 + \frac{4}{3}Sr(OH)_2$
$2SrCrO_4 + \frac{4}{3}Sr(OH)_2 \longrightarrow \frac{2}{3}Sr_5(CrO_4)_3OH + H_2O + \frac{1}{2}O_2$
H_2O
$\frac{1}{2}O_2$

A PROMISING THERMOCHEMICAL CYCLE FOR SPLITTING WATER

Bernard M. Abraham, Felix Schreiner, Alan Attia , and Anthony Jeanotte

CHEMISTRY DIVISION./ARGONNE NATIONAL LABORATORY, Argonne, IL 60439

The continued search at Argonne National Laboratory for a process by which water can be decomposed thermochemically has led to the development of a reaction sequence that requires a maximum temperature no higher than 900 K. The cycle has been designated ANL-4 and consists of the following reactions:

$$2H_2O + 2NH_3 + 2CO_2 + 2KI \xrightarrow[\text{solution}]{T = 300\text{ K}} 2KHCO_3 + 2NH_4I \qquad (4\text{-}1)$$

$$2KHCO_3 \xrightarrow{T = 425\text{ K}} K_2CO_3 + CO_2 + H_2O \qquad (4\text{-}2)$$

$$2NH_4I + Hg \xrightarrow{T = 700\text{ K}} H_2 + 2NH_3 + HgI_2 \qquad (4\text{-}3)$$

$$K_2CO_3 + HgI_2 \xrightarrow{T = 900\text{ K}} 2KI + Hg + CO_2 + 1/2\ O_2 \qquad (4\text{-}4)$$

The sum of reactions (4-1) - (4-4) is the splitting of one mole of liquid H_2O

$$H_2O \rightarrow H_2 + 1/2\ O_2$$

The thermodynamic analysis of this scheme shows it as potentially being capable of converting nearly 60% of the high-temperature heat into chemical potential energy, and laboratory experimentation indicates favorable rates and yields for the important high-temperature reactions. The process flow diagram brings out the advantageous feature of the cycle that most of the reactants and products can be handled as gases, melts, or as solutions. There remain certain problem areas such as the comparatively low separation efficiency of reaction (4-1) which necessitates the recycling of relatively large volumes of solutions and the presence of mercury in the effluent gases from reaction (4-4).

These reactions require additional work; nonetheless, there is good reason to believe that further development will be successful in improving the cycle.

It has been shown previously that the principal thermodynamic characteristics of a cycle are conveniently represented by a diagram of entropy versus temperature (3). Such a diagram for the cycle ANL-4 is shown in Figure 1 which was constructed from the data listed in Table 1. For the most part the numbers were taken from tables of "Thermochemical Properties of Inorganic Substances" by Barin and Knacke(4). In the case of potassium hydrogen carbonate the required quantities were calculated from the dissociation pressure curve(5) or estimated by comparison with sodium hydrogen carbonate.

The closed-loop trace of the entropy-temperature diagram represents the entropy changes of reactants and products during traversal of the complete water decomposition cycle according to the reactions (4-1) through (4-4). In order to close the loop thereby indicating that the entire system has been returned to the initial physical state, the entropy of formation of liquid water is included. The numerical values used in the drawing of Figure 1 refer to the splitting and recombination of one mole of water so that the area enclosed by the loop represents the Gibbs energy of formation for one mole of water at 298.15 K (237.2 kJ).

The sign of the entropy change for each reaction is indicated by the direction of the arrow. The temperatures at which the arrows for the respective reactions are plotted are the temperatures at which the Gibbs energies are zero, with the exception of the arrow representing the re-formation of water at 298.15 K.

Three of the reactions, (4-2), (4-3), and (4-4) absorb heat, which must be furnished from the primary source. The minimal thermodynamic heat requirement for this water decomposition cycle is 5.27 kJ. The efficiency of the cycle, in turn, is expressed in the usual manner by the ratio of the chemical potential energy, i.e., the Gibbs energy of formation of the water, to the heat requirement. For the cycle ANL-4 this ratio is $\eta_{ANL-4,\ ideal}=0.45$. The temperature of the primary heat source furnishing the energy for the water splitting process must be high enough to permit the reaction (4-4) to proceed, that is to say it must be at least 810.8 K. A classical Carnot-type heat engine operating between this temperature and ambient would be capable of converting 63% of the heat into useful work.

Three of the reactions making up the water decomposition cycle ANL-4 were studied in the laboratory in order to check the general chemistry, to verify the results of the thermodynamic calculations, and to demonstrate adequacy of reaction rates. They include the reaction (4-1), and the two high-temperature reactions (4-3) and (4-4).

Reaction (4-1) involves the conversion of potassium iodide into potassium hydrogen carbonate in a solvent medium. Unfortunately, it is not possible to use water alone for the solvent as can be done so successfully in the case of sodium salts. However, with mixtures of organic solvents and water it is possible to achieve the conversion to an adequate extent. The data listed in Table 2 support this conclusion. They were obtained by heating equimolar mixtures of ammonium hydrogen carbonate and potassium iodide with the solvents to near boiling temperature, at which point the ammonium hydrogen carbonate is not stable. It was quickly established that the mixtures had to be pressurized either with mixtures of ammonia and carbon dioxide or with carbon dioxide alone, in order to improve the conversion efficiency. Samples from the saturated solutions were taken after equilibration and cooling to ambient temperature, and analyzed chemically.

The comparatively short series of experiments with a variety of solvent mixtures led to workable levels of salt interconversion with a 87.5% aqueous isopropanol solution under pressure of 50 psi of carbon dioxide.

The salt composition in that solution after equilibration corresponds to a mixture of 77% of ammonium iodide, 16% of potassium iodide, and of 7% of potassium hydrogen carbonate. It is very likely that still better systems can be found by further experimentation, but for the purpose of the present study the 7:1 isopropanol - water mixture was considered satisfactory.

The two high temperature reactions (4-3) and (4-4) were found to be straightforward and to proceed in accordance with the respective equations.

They are not encumbered by side reactions that lower product yields. It was also found that the equilibrium temperatures calculated from literature data are close to the observed values. Experimental results of the measurement of the reaction

$$2NH_4I + Hg = Hg + 2NH_3 + H_2$$

are summarized in Table 3. These numbers were obtained by enclosing known quantities of ammonium iodide and mercury in a cylindrical reaction vessel made of fused silica. The vessel had a diameter of about 50 mm and a volume of approximately 300 cm^3. It was loaded with the reactants, sealed under vaccum, then placed in a furnace and heated to the experimental temperature. After an equilibration time of up to one hour the vessel was removed from the furnace and cooled quickly. For analysis of the products, the vessel was attached to a pumping line by way of a breakseal. The gaseous products were separated by fractional condensation at 77 K and at 195 K (solid CO_2). The gases were transferred into known volumes with a Toepler pump and the pressure determined with a fused quartz Bourdon gage. To identify the products, samples were taken for mass-spectrometric analysis. The analysis showed the gases to have the composition expected from the equation; and no evidence for the decomposition of ammonia was found.

In addition to the measurement of equilibrium constants the rates of the reaction (4-3) were determined. In this case, the fused silica reaction vessel was equipped with optical windows which were recessed by approximately 5 cm in re-entrant wells at both ends. It was possible by this precaution to avoid condensation of mercury or mercury iodide vapor on the windows. The reaction rates at various temperatures were determined by following the build-up of mercuric iodide vapor photometrically. The reaction vessel was charged with a known quantity of NH_4I and a known quantity of Hg contained in an evacuated soft glass ampoule. The reaction was initiated at the experimental temperature by fusing the ampoule located in a side arm of the reaction vessel so the Hg vapor could contact the vaporized NH_4I

The observed rate at 680 K was proportional to the concentration of mercury and the concentration of ammonium iodide, and the second order rate constant has the value

$$k = 1.7 \pm 0.1_3 \text{ lit/s/mole.}$$

The half time for the reaction is $t_{1/2}$ = 2.3 minutes at moderate experimental pressures of $\sim$ 0.5 atm for the initial pressure of HI.

Measurements of equilibrium constants were also carried out for reaction (4-4). Rate measurements have not been made but qualitatively the reaction seems rapid. In this case, too, it was found that the calculated numbers agreed well with the experimental data. Since potassium carbonate at high temperatures attacks the fused silica, the solid reactants were contained in a magnesia crucible and the reaction vessel was mounted vertically.

A mixture of 2.2 mmol of HgI and 7.24 mmol of K_2CO_3 evolved 1.08 mmol of oxygen at 899 K; this corresponds to 98% reaction. The experimental Kp = 13.4 and the calculated Kp = 12.4.

The conclusions from the experimental investigation of the reaction of the cycle ANL-4 can be summarized as follows: All reactions can be carried out under conditions under which reasonably rapid rates are obtained and the yields of the high-temperature reactions are essentially 100%. The highest temperature required is 900 K. The chemistry of the reactions follows the equations (4-1) through (4-4) and there are no harmful side reactions. In particular, no decomposition of any of the ammonia was observed with reaction (4-3). With respect to yields, reaction (4-1) is the least attractive one, and since the overall solubility is not very high in the isopropanol mixture appreciable volumes of solution have to be cycled during the process. However, the solution need never be handled at very high temperatures, and waste heat from extraneous sources might be used to make up losses that cannot be recovered by a system of heat exchangers.

The movement of energy, reactants and products of the cycle ANL-4 are shown in the flow diagram Figure 2. There are, broadly speaking, three major sections in this diagram. On the left hand side there is a column representing from top to bottom the operations concerned with the recovery and calcination of potassium hydrogen carbonate and the subsequent reaction during which oxygen is released. A similar column on the right hand side shows the operations of recovering the ammonium iodide from solution and of producing the hydrogen in the reaction of NH_4I with mercury. Finally, surrounding the two vertical sections is a peripheral loop representing the circulation of solution or slurry.

Primary heat is furnished to the reactors at R42, R44, and R43 (a certain small fraction of heat, also indicated as stemming from the primary source, is used to dry the ammonium iodide). The water feed enters the process as make-up water in the scrubber which removes the ammonia from the product hydrogen. The ammoniacal solution containing a residual amount of iodide is moved clockwise into a second scrubber where it is pressurized with carbon dioxide at the same time that the oxygen leaves the process. Potassium iodide is added and the resultant slurry is heated to near boiling point temperature. The heating occurs in two steps the second one making use of the heat content in the effluent from the oxygen reactor.

The hot slurry now contains the iodide in solution and is transferred into a settling tank where the potassium hydrogen carbonate is separated. The solid is forwarded to the calcinating furnace and further into the potassium carbonate reactor, R44. Here it is brought to react with mercury iodide vapor which is fed across from the ammonium iodide reactor, R43. The products from the carbonate reactor then enter the solution-slurry circuit, except for the oxygen which is vented.

The solution from the potassium hydrogen carbonate settling tank is cooled to ambient temperature and turned into a slurry of ammonium iodide. Some of the heat removed during this process is used to heat the slurry at a preceeding stage in order to conserve heat. The ammonium iodide is separated from the dilute solution, dried, and passed on into the iodide reactor, R43. It reacts with mercury coming from the carbonate reactor, R44, and forms mercury iodide, ammonia, and the principal product, hydrogen. Mercury iodide is collected as a liquid to be used in the reactor R44, ammonia is scrubbed, and the hydrogen is collected.

The flow of reactants, the pattern of heat exchange and use of primary heat outlined here permits an estimate of the basic heat requirement for the cycle.

Primary heat is assumed to be used for the high-temperature reactions (4-3) and (4-4), for the calcination of the hydrogen carbonate, and to make up for losses not recoverable by heat exchangers. Direct losses of heat to the environment from the reactors and transfer lines because of imperfect insulation were not considered. A summary of the numbers used for the estimate is contained in Table 4. With reasonable assumptions about the efficiency of the heat exchange systems the total amount of heat that has to be supplied is 930 kilojoules per mol of hydrogen produced.

This result corresponds to an overall efficiency of heat converted into chemical potential energy (i.e. referred to the Gibbs energy of formation of water) of

$$\eta_{ANL-4} = 0.255$$

Though this number may seem small by comparison to the ideal value it is nevertheless respectable when compared to electrolysis, the only process by which hydrogen can be made without reliance on fossil fuels. Besides, it was arrived at as an overall efficiency based on a flow pattern reflecting the actual conditions under which the process can be conducted in a realistic manner.

In addition to the reasonable heat conversion efficiency the cycle ANL-4 has a number of attractive features. These include the clean chemistry of the important reactions, the low maximum temperature of 900 K, and the fact that the reactants permit efficient handling as liquids and slurries.

Against this stands the presence of mercury which may require special treatment of effluents, and the large volume of solvent that needs to be circulated. However, we believe this cycle is suitable to demonstrate the concept of thermochemical water splitting and offers the opportunity to acquire necessary information for reactor and heat exchanger design.

ACKNOWLEDGEMENT

We wish to thank Mr. Michael Grimm, Student Aide, for performing the chemical ayalyses.

Table 1. Entropy balance for the cycle ANL-4.

Operation	Entropy change[a] $\Delta S_{reaction}$ or $\int \frac{\Delta Cp}{T}\,dt$ $J \cdot K^{-1}$	Entropy of the system $J \cdot K^{-1}$
Heating of H_2O	$\int_{298.2}^{327.2} \frac{Cp}{T}\,dT = + 7.0$	+ 7.0
Reaction (4-1) at 327.2 K	$\Delta S = - 683.6$	- 676.6
Heating of $2KHCO_3 + 2NH_4I$	$\int_{327.2}^{430.1} \frac{\Sigma Cp}{T}\,dT = + 104.0$	- 572.6
Reaction (4-2) at 430.1 K	$\Delta S = + 300.0$	- 272.6
Heating of $K_2CO_3 + 2NH_4I$	$\int_{430.1}^{538.4} \frac{\Sigma Cp}{T}\,dT = + 72.8$	- 199.8
Reaction (4-3) at 538.4	$\Delta S = + 413.4$	+ 213.6
Heating of $K_2CO_3 + HgI_2$	$\int_{538.4}^{810.8} \frac{\Sigma Cp}{T}\,dT = + 88.8$	+ 302.4
Reaction (4-4) at 810.8	$\Delta S = + 209.0$	+ 511.4
Cooling of $2KI + Hg + CO_2 + 1/2\ O_2$	$\int_{810.8}^{538.4} \frac{\Sigma Cp}{T}\,dT = - 84.6$	+ 426.8
Cooling of $2KI + 2NH_3 + CO_2 + H_2 + 1/2\ O_2$	$\int_{538.4}^{430.1} \frac{\Sigma Cp}{T}\,dT = - 64.2$	+ 362.6
Cooling of $2KI + 2NH_3 + 2CO_2 + H_2O + H_2 + 1/2\ O_2$	$\int_{430.1}^{373} \frac{\Sigma Cp}{T}\,dT = - 50.0$	+ 312.6
Condensation of H_2O at 373 K	$\Delta S = - 110.4$	+ 202.2
Cooling of $2KI + 2NH_3 + 2CO_2 + H_2O + H_2 + 1/2\ O_2$	$\int_{373}^{327.2} \frac{\Sigma Cp}{T}\,dT = - 51.2$	+ 151.0
Cooling of $H_2 + 1/2\ O_2$	$\int_{327.2}^{298.2} \frac{\Sigma Cp}{T}\,dT = - 7.8$	+ 143.2
Reaction $H_2 + 1/2\ O_2 = H_2O$ at 298.2 K	$\Delta S = - 143.2$	0.0

[a] The calculated entropy changes were individually adjusted by no more than 1.3% to obtain overall balance for the cycle.

Table 2. Solution behavior of mixtures of KI and NH_4HCO_3 in various solvents

(Sampling temperature: 298.2 K)

Solvent	Gas atmosphere	Cation ratio NH_4^+/K^+	Anion ratio I^-/HCO_3^-	Concentration of solute mol/1000g solvent
H_2O	air, 1 atm	1.1	3.5	7.6
H_2O	air, 1 atm	1.1	1.8	8.5
Ethanol-H_2O 3:1	NH_3+CO_2, 3.7 atm	1.7	11.7	1.8
Ethanol-H_2O 7:1	CO_2, 3.9 atm	0.7	25.0	1.0
Isopropanol-H_2O 3:1	CO_2, 4.9 atm	2.1	11.8	1.8
Isopropanol-H_2O 7:1	CO_2, 4.4 atm	3.4	13.9	0.7

Table 3. Equilibrium constants for the reaction $2NH_4I(g) + Hg(g) \rightleftharpoons 2NH_3 + HgI_2(g) + H_2$

Temperature K	Initial charge mmol NH_4I	Hg	Amount H_2 recovered mmol	Kp experimental	Kp calculated
731	3.26	4.49	1.59	1011	936
783	2.90	5.28	1.39	216	225

Table 4. Heat tally for cycle ANL-4.

	Heat required kilojoules	Heat supplied from primary source kilojoules	Heat recovered through heat exchanger systems kilojoules
Reaction (4-1)	475	0	475
Drying & heating of $KHCO_3$	105	105	0
Reaction (4-2)	135	135	0
Vaporization of Hg	70	2	68
Drying of NH_4I	99	99	0
Heating of NH_4I	123	123	0
Reaction (4-3)	235	235	0
Vaporization of HgI_2	104	34	70
Heating of K_2CO_3	84	84	0
Reaction (4-4)	175	175	0
Total heat	1543	930	613

Efficiency of conversion: $\eta_{ANL-4} = \frac{237}{930} = 0.255$

References

1. Work performed under the auspices of the U. S. Energy Research and Development Administration.

2. Present address: Wright-Patterson AFB Dayton, Ohio.

3. B. M. Abraham and F. Schreiner, Ind. Eng. Chem., Fundam., 13, 305 (1974).

4. I. Barin and O. Knacke, Thermochemical Properties of Inorganic Substances, Springer-Verlag, New York, 1973.

5. R. M. Caven and H. J. Sand, J. Chem. Soc., 105, 2753 (1914).

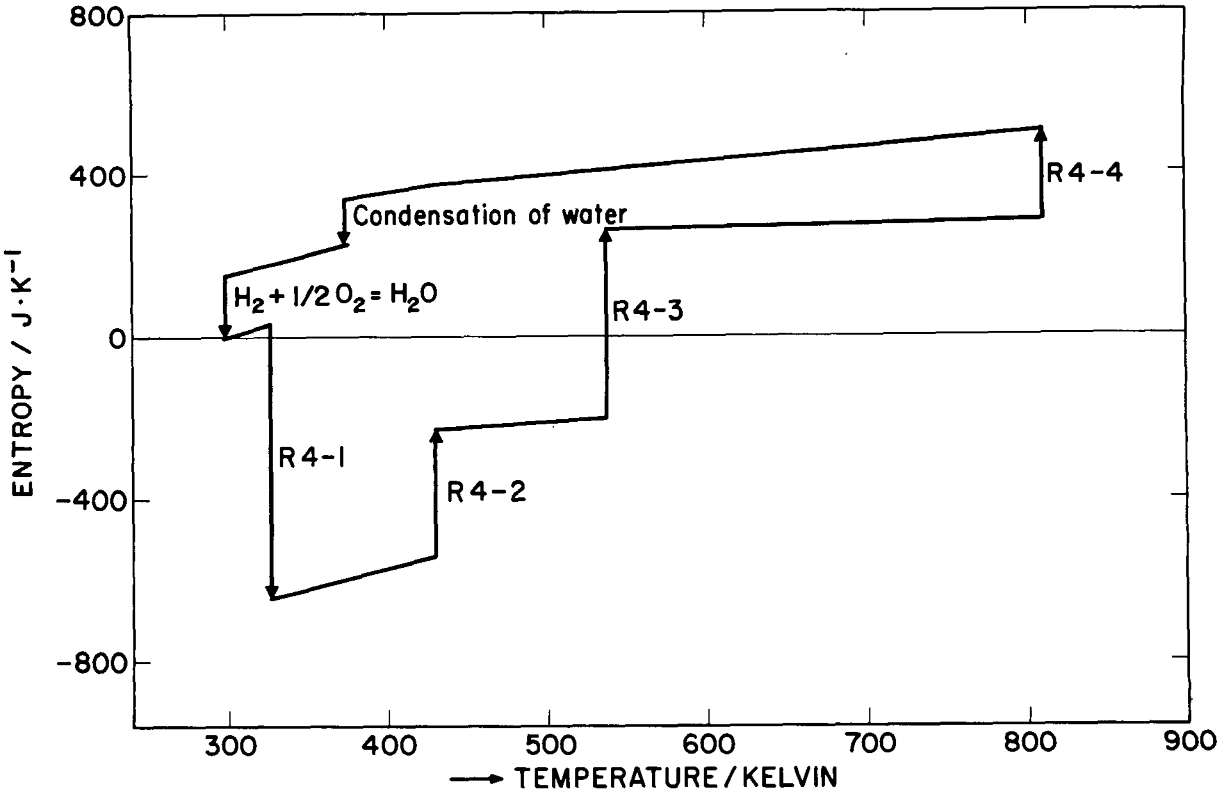

Figure 1. Entropy-temperature diagram for thermochemical water splitting cycle ANL-4. The area enclosed by the diagram equals the Gibbs energy for the decomposition of water into the elements at the standard states.

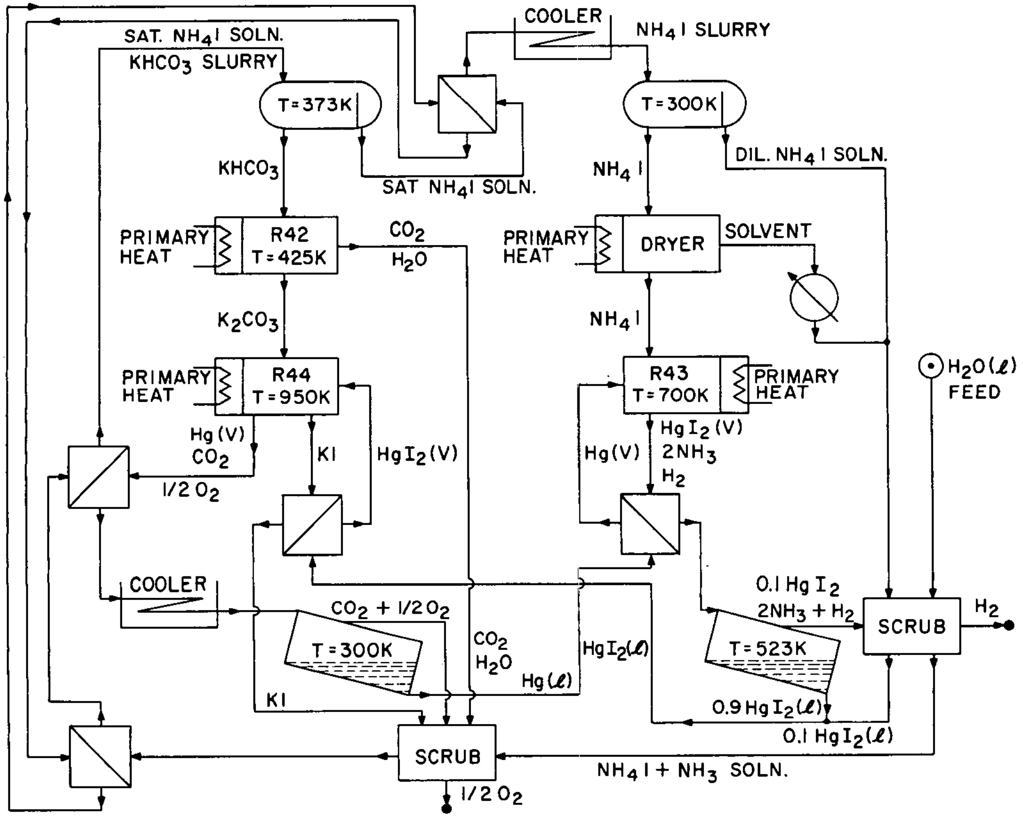
SAT. NH_4I SOLN.
$KHCO_3$ SLURRY
COOLER
NH_4I SLURRY
T=373K
T=300K
$KHCO_3$
SAT NH_4I SOLN.
NH_4I
DIL. NH_4I SOLN.
PRIMARY HEAT
R42 T=425K
CO_2
H_2O
PRIMARY HEAT
DRYER
SOLVENT
K_2CO_3
NH_4I
PRIMARY HEAT
R44 T=950K
R43 T=700K
PRIMARY HEAT
$H_2O(\ell)$ FEED
Hg(V)
CO_2
KI
$HgI_2(V)$
Hg(V)
$HgI_2(V)$
$2NH_3$
H_2
1/2 O_2
COOLER
CO_2 + 1/2 O_2
T=300K
CO_2
H_2O
Hg(ℓ)
$HgI_2(\ell)$
0.1 HgI_2
$2NH_3 + H_2$
T=523K
SCRUB
H_2
KI
0.9 $HgI_2(\ell)$
0.1 $HgI_2(\ell)$
SCRUB
$NH_4I + NH_3$ SOLN.
1/2 O_2

Figure 2. Flow diagram for thermochemical water splitting cycle, ANL-4

THE DESIGN AND ECONOMICS OF A NUCLEAR-POWERED WATER DECOMPOSITION SYSTEM FOR HYDROGEN GENERATION, G.H. Farbman, L.E. Brecher, D. Bogart, Westinghouse Electric Corporation, Pittsburgh, PA.

A conceptual design of a nuclear water decomposition system. Operating characteristics, process flow diagrams, and plant arrangement drawings are presented.

BASIC CHEMISTRY IN THE IDENTIFICATION AND EVALUATION OF THERMOCHEMICAL CYCLES FOR HYDROGEN PRODUCTION FROM WATER. Melvin G. Bowman, Los Alamos Scientific Laboratory, Los Alamos, NM 87545.

There is an existing and rapidly expanding market for hydrogen at present. Eventually, production of hydrogen from fossil fuels must be supplemented by large volume production from alternate energy sources. It is probable that such production will utilize nuclear and/or solar energy for the decomposition of water by electrolysis or by thermochemical methods. The inherent higher efficiency and potentially lower cost for thermochemical methods, versus the overall electrolysis path, can be demonstrated. However, realization will require the identification and development of cycles of chemical reactions that approximate the thermodynamic and chemical criteria that define an ideal cycle. These criteria include: (1) Enthalpy changes (ΔH^o) and entropy changes (ΔS^o) for reactions in the cycle should approximate those dictated by the free energy of formation of water and by the high temperature heat available for the endothermic reactions. For known and projected heat sources, rather large ΔS^o values are required in order for ΔG^o to be zero with a minimum number of reactions. This implies that the reactions should yield gaseous products. (2) Gaseous reaction products (except for H_2 and O_2) should condense above ambient temperatures in order to minimize separation work. (3) Side reactions or competing reactions must be unimportant. Thus, ΔG^o values for all potential reactions must be evaluated. (4) Reaction rates for the desired reaction must be sufficiently rapid for practical heat exchangers. Examination of many proposed thermochemical cycles reveals that most do not approximate the above criteria.

EXPERIMENTAL AND THEORETICAL INVESTIGATION OF THERMOCHEMICAL HYDROGEN PRODUCTION, K. F. Knoche, Lehrstuhl Für Technische Thermodynamik, Aachen, Germany.

A report of experimental and theoretical investigations of hydrogen production by thermo-chemical cycles.

THERMAL DECOMPOSITION OF SOME METAL SULFATES

K. H. Lau, D. L. Hildenbrand, and D. Cubicciotti

Stanford Research Institute
Menlo Park, California 94025

A number of thermochemical cycles for producing hydrogen from water are based on sulfate systems (1). A simple cycle, for example, is:

$$MgSO_4 \rightarrow MgO + SO_2 + 1/2O_2 \qquad 1400\ K$$

$$MgO + H_2O + S + SO_2 \rightarrow MgSO_4 + H_2S \qquad 500\ K$$

$$H_2S \rightarrow H_2 + S \qquad 1400\ K$$

The predicted efficiency for conversion of primary heat into chemical energy in the form of hydrogen by such a cycle is very sensitive to the quality of the thermodynamic data used in evaluating each step. Errors of several kcal in a reaction enthalpy, for example, can effect a change of several percentage points in a calculated efficiency (2, 3). A close inspection of available data shows that the thermodynamics of some sulfate cycle steps are not known with sufficient accuracy to rank the cycles properly. Additionally, it is doubtful that many of the steps proceed as written because of side reactions, condensed phase interactions, kinetic limitations, and so on.

We are studying the high temperature chemistry of metal sulfate decomposition processes on a program funded by the National Science Foundation. This decomposition step, typified by the reaction $MSO_4(s) \rightarrow MO(s) + SO_2(g) + 1/2O_2(g)$, is common to all sulfate cycles, as exemplified in the cycle referred to earlier. However, the thermochemistry of many metal sulfates is not well established, and directly measured decomposition pressures are often inconsistent or incomplete. Both of these sources of error are stressed in reviews of sulfate decomposition equilibria (4, 5). Information about the kinetics of these decompositions is also crucial to the development of efficient cycles; again the available data are fragmentary (4). The objective of our program is to provide some of the fundamental thermochemical and kinetic data required in the overall evaluation of sulfate cycles.

At this stage, detailed studies of the vaporization-decomposition of $MgSO_4$ and $CaSO_4$ have been carried out by means of the combined torsion and gravimetric Knudsen effusion method. With this method, one measures simultaneously the recoil force and the weight loss associated with the molecular effusion process, and can thereby evaluate both the vapor pressure and vapor molecular weight of the substance being studied. A description of the torsion method and its application to various vaporization studies is given in previous publications (6-8). In addition, the vaporization of $MgSO_4$ was also studied by high temperature mass spectrometry, using an instrument and technique described in earlier work (9, 10). Alumina effusion cells were used in all of the present studies. Results obtained on $MgSO_4$ and $CaSO_4$ are described separately below.

A. $MgSO_4$

Torsion-gravimetric effusion measurements were made with four cells of orifice diameter 0.6, 1.0, 1.5, and 2.00 mm covering a range of 980 to 1060 K. A substantial variation of decomposition pressure with effective orifice area (product of orifice area and transmission factor) was observed, indicating an appreciable kinetic barrier for the vaporization-decomposition process.

Additionally, the measured vapor molecular weight, M^*, showed an interesting variation with temperature and orifice area. M^* derived from the combined torsion-weight loss data is really a weight average molecular weight, and would have values of 54.6 and 80.1 for the overall vaporization processes $MgSO_4(s) = MgO(s) + SO_2(g) + 1/2O_2(g)$ and $MgSO_4(s) = MgO(s) + SO_3(g)$, respectively. With the larger orifices at the lower end of the temperature range, M^* values of 78-80 were measured, indicating the vapor to be comprised almost entirely of SO_3 under those conditions. Vapor molecular weights determined with the 0.6 and 1.0 mm diameter orifice cells were somewhat lower, varying from 55 to 65 $[P(SO_3)/P(SO_2) = 0.02$ to $0.92]$, a clear indication that vapor composition is approaching the $SO_2 + 1/2O_2$ stoichiometry as orifice size decreases, and as temperature and residence time of gaseous species in the cell increase. Since a free energy calculation shows that at equilibrium the ratio $P(SO_3)/P(SO_2) < 100$ under our conditions, it is obvious that the vaporization process is kinetically limited to a substantial degree. It is a matter of both practical and fundamental importance to determine the nature of this kinetic barrier.

As a check on the vapor molecular weights, the composition of the effusing vapor over $MgSO_4(s)$ was determined by high temperature mass spectrometry, using an alumina cell with 1.5 mm diameter orifice. Over the range 940 to 1080 K, the ratio $P(SO_3)/P(SO_2)$ was found to have the relatively constant value of 19 ± 1. In agreement with the above molecular weight measurements. The mass spectrometric data thus reinforce the concept of a kinetically limited vaporization process. It appears that under dynamic conditions, the initial vaporization step involves the evolution of an SO_3 molecule, rather than the equilibrium mixture of SO_2 and O_2 on the surface. There are several factors which could influence the kinetics of the final conversion to SO_2 and O_2, including the thickness of the residual MgO layer on the sample, possible catalytic effects of the sample surface and/or cell walls, and the temperature.

A thermodynamic analysis of the results reveals other interesting information. Figure 1 is a plot of our measured total pressures for the $MgSO_4$ decomposition, obtained by the torsion method with the 0.6 and 1.0 mm diameter orifices. The solid line in Figure 1 is the pressure derived from these data by an extrapolation to zero orifice area using the Whitman-Motzfeldt relation $P_e = P_T(1 + BCa)$ where P_e and P_T are equilibrium and observed pressures, C and a are orifice area and Clausing factor, and B is a constant for a particular cell design. It would be especially instructive to compare the extrapolated pressures with calculated equilibrium pressures for the process $MgSO_4(s) = MgO(s) + SO_2(g) + 1/2O_2(g)$, since measured M^* values are approaching the $SO_2 + O_2$ composition at the temperature shown. However, the heat of formation and heat content of $MgSO_4$ are not sufficiently well established for a meaningful thermodynamic calculation of equilibrium pressures. Shown, instead, in Figure 1 are equilibrium pressures extrapolated from the higher temperature decomposition measurements of Dewing and Richardson (11) and from the selected data of Kellogg (4). Our derived pressures extrapolated to zero orifice area are an order of magnitude or more lower than the best literature results for the equilibrium decomposition process, further evidence of a severe kinetic limitation. Much remains to be done to clarify the situation, but a tentative explanation envisions SO_3 as the primary vaporizing species, with subsequent decomposition to SO_2 and O_2 by wall, surface or gas phase collisions, the extent of which is highly dependent on residence time. A measured M^* close to 55 would not necessarily signify total equilibration within the cell, but could be the result of a large concentration gradient between sample surface and effusion orifice. In this sense, the observed pressure would be dominated by the evolution of SO_3.

It appears that the pressure data obtained with the larger effusion orifices, where vapor molecular weights of 80 ± 2 indicate the vapor to be composed largely of SO_3, can be interpreted to yield the SO_3 equilibrium decomposition pressure for the process $MgSO_4(s) = MgO(s) + SO_3(g)$, which can be used in turn to derive a value for the enthalpy of formation of $MgSO_4(s)$. Our preliminary analysis yields $\Delta Hf^o_{298}(MgSO_4) = -311 \pm 1$ kcal/mol, and indicates the JANAF Table (12) value to be in error by about 10 kcal/mol.

B. $\underline{CaSO_4}$

Because of the complex results observed for $MgSO_4$, it seemed worthwhile to test the applicability of the effusion method and the Whitman-Motzfeldt model to a sulfate decomposition process for which all the relevant thermodynamic data are reasonably well established. $CaSO_4$ is highly satisfactory in this regard, and to our knowledge, there are no previous effusion measurements reported.

To date, torsion pressure data and vapor molecular weights have been obtained over the range 1140 to 1240 K with effusion cells of 0.6 and 1.0 mm diameter orifice area. A plot of the observed pressure data is shown in Figure 2. With both cells, M^* values of 54 ± 2 were determined, independent of temperature, clearly indicating the effusing vapor to have the stoichiometry $SO_2 + 1/2O_2$. Also shown as the solid line on Figure 2 is the pressure derived from a zero orifice size extrapolation and its comparison with the selected equilibrium data of Kellogg (8) and equilibrium pressures calculated from thermochemical data for the process $CaSO_4(c) = CaO(c) + SO_2(g) + 1/2O_2(g)$.

It is evident that the extrapolated effusion pressures agree closely with the best available equilibrium data, providing a satisfactory test of the experimental technique and data treatment model. The observed orifice size effect does signify an appreciable kinetic barrier, but in this instance it would appear that the barrier does not include a slow $SO_3 \rightarrow SO_2$ conversion step on the surface or on the walls. In contrast to the results for $MgSO_4$, this behavior of $CaSO_4$ may be due to enhanced catalytic properties of the $CaSO_4$ - CaO surface, or to a simple temperature effect. (The $CaSO_4$ measurements were made at temperatures about 200 degrees higher than for $MgSO_4$.)

C. Mechanism of Decomposition

Although the experimental and data analysis phases of the work on $MgSO_4$ and $CaSO_4$ are not yet complete, we present here some preliminary thoughts about the mechanism of sulfate decomposition.

The effusion results obtained to date can be interpreted to indicate that the first step in the decomposition of $MgSO_4$ is:

$$MgSO_4(s) \rightarrow MgO(s) + SO_3(g) \qquad 1)$$

even though the thermodynamically favored reaction is decomposition to $SO_2 + O_2$. Reaction 1) is then followed by further decomposition

$$SO_3(g) \rightarrow SO_2(g) + 1/2O_2(g) \qquad 2)$$

only if the SO_3 has sufficient residence time in the effusion cell. In other words, reaction 2) is catalyzed by processes occurring inside the effusion cell, and the longer SO_3 residence times associated with the smaller orifices lead to the observed decrease in the ratio $P(SO_3)/P(SO_2)$.

The results are in accord with the literature. Hulbert (13) studied the kinetics of decomposition of $MgSO_4$ between 920° and 1080°C, and found that the results could be represented by a contracting-sphere rate equation, which implies that the rate is controlled by the surface area of unreacted $MgSO_4$. That is, the rate per unit surface area is constant, but the amount of surface decreases as the particles decompose. The activation energy was 74.5 kcal per mole, which is close to the enthalpy change for reaction 1), 72 ± 5 kcal/mole, implying that reaction 1) is rate-limiting. The effect of sample size was interpreted as indicating that increased SO_3 pressure decreased the rate. That is, further evidence that reaction 1) is rate limiting. Pechkovski (14, 15) found that, in a stream of flowing gas at temperatures of 750 to 1050°C, the rate of decomposition of $MgSO_4$ was independent of the partial pressure of O_2. That result also indicated reaction 1) was the rate limiting step rather than the thermodynamically more favored reaction 3)

$$MgSO_4(s) \rightarrow MgO(s) + SO_2(g) + 1/2O_2(g) \qquad 3)$$

for which the rate would be inhibited by oxygen. Knopf and Staude (16) quenched a gas stream that had passed over heated $MgSO_4$ and identified SO_3 as a product, which indicates that reaction 2) was slower than reaction 1) in their experiments.

On the other hand, our results show that in the decomposition of $CaSO_4$ the products are SO_2 and O_2, independent of temperature and orifice size. Searcy and his students have studied the decomposition of $BaSO_4$ (17) and $SrSO_4$ (18). They found the decomposition products to be SO_2 and O_2, and their torsion effusion results for $BaSO_4$ were in agreement with equilibrium pressures calculated from thermodynamic data for the reaction analogous to reaction 3).

Searcy's group has also measured the rate of evaporation of $BaSO_4$ under free surface conditions. Under those conditions, the apparent pressures are about 1% of the equilibrium values. They remark that their explanation, in terms of active surface sites, is not entirely satisfactory.

We feel that the behavior of $MgSO_4$ compared to the sulfates of Ca, Ba, and Sr can be explained by a different model, as follows. The rate determining step is presumed to be the surface desorption of SO_3 for all these sulfates. The metal oxide formed by the decomposition is left on the surface as a porous layer which does not impede the desorption of SO_3. However, as the SO_3 diffuses through the oxide layer it is converted to SO_2 and O_2. In effect, the porous oxide layer catalyzes the conversion of SO_3 to SO_2 and O_2. Catalysis by the MgO layer is presumed to be much less effective than that by CaO, SrO or BaO; therefore, the apparent products of the reaction are SO_3 for $MgSO_4$ and SO_2 and O_2 for the other sulfates.

The reason that MgO is less catalytic may be simply that the temperature is lower for MgO than the other oxides by several hundred degrees. The decomposition of SO_3 is a thermally activated reaction (19) (activation energy, 40 kcal per mole). There is also some evidence that the decomposition of $MgSO_4$ is catalyzed by oxides, i.e., Fe_2O_3, Cr_2O_3 and CuO (14, 15).

These initial studies indicate that the experimental method can be used to generate thermodynamic data needed in cycle analysis, and also that the kinetics of the decomposition process may present some practical problems. In particular, the conversion of SO_3 to $SO_2 + O_2$ may be a rate limiting step in low temperature sulfate decompositions. Further studies of the thermodynamics and kinetics of sulfate decompositions are in progress.

REFERENCES

1. M. A. Soliman, R. H. Carty, W. L. Conger, and J. E. Funk, Can. J. Chem. Eng. 53, 164 (1975).

2. J. B. Pangborn and D. P. Gregory, "Nuclear Energy Requirements for Hydrogen Production from Water," 9th Intersociety Energy Conversion Engineering Conference, San Francisco, August, 1974.

3. J. B. Pangborn, personal communication.

4. H. H. Kellogg, Trans. Met. Soc. AIME 230, 1622 (1964).

5. K. H. Stern and E. L. Weise, NSRDS-NBS-7, U.S. Govt. Printing Office, Washington, D.C. (1966).

6. D. L. Hildenbrand and W. F. Hall, J. Phys. Chem. 67, 888 (1963).

7. D. L. Hildenbrand, W. F. Hall, and N. D. Potter, Jr. Chem. Phys. 39, 296 (1963).

8. D. L. Hildenbrand and D. T. Knight, J. Chem. Phys. 51, 1260 (1969).

9. D. L. Hildenbrand, J. Chem. Phys. 48, 3657 (1968); 52, 5751 (1970).

10. D. L. Hildenbrand, Int. J. Mass Spectrom. Ion Phys. 4, 75 (1970); 7, 255 (1961).

11. E. W. Dewing and F. D. Richardson, Trans. Farad, Soc. 55, 611 (1959).

12. JANAF Thermochemical Tables, The Dow Chemical Co., Midland, Mich., revision of June, 1975.

13. S. F. Hulbert, Mat. Sci. Eng., 2, 262, (1968).

14. V. V. Pechkovski, Sh. Prikl. Khim., 29, 1137 (1956).

15. V. V. Pechkovski, Uch. Zap. Perusk. Gos. Univ. 13, 93 (1959).

16. H. J. Knopf and H. Staude, Z. Physik. Chem. 204, 265 (1955).

17. P. Mohazzobi and A. W. Searcy, Kinetics and Thermodynamics of Decomposition of Barium Sulfate, Lawrence Berkeley Laboratory, Report No. LBL, 3773, 1975.

18. Fuke, Dissertation with Professor A. W. Searcy, Lawrence Berkeley Laboratory, Report No. LBL 1832, 1973.

19. G. B. Taylor and S. Lenher, Z. Physik. Chem., Bodenstein Festband, 30 (1931).

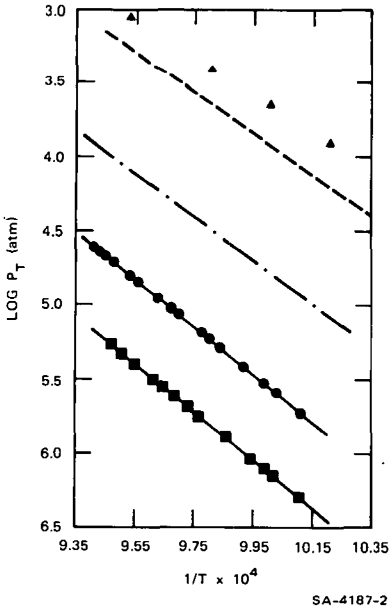

FIGURE 1 VAPOR PRESSURE OF MAGNESIUM SULFATE;

■ Cell 3 ● Cell 4

▲ Dewing and Richardson Data

—·— Extrapolation to Zero Orifice Area

– – – Kellogg's Data

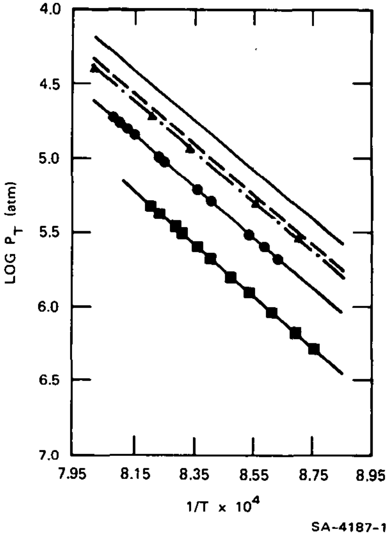

FIGURE 2 VAPOR PRESSURE OF CALCIUM SULFATE;

■ Cell 3 ● Cell 4

▲ Dewing and Richardson Data

—·— Extrapolation to Zero Orifice Area

– – – Kellogg's Data

—— Kelley's Data

Thermochemical Water Splitting: The Reverse Deacon Reaction and Alternatives*

Ulrichson, Dean L. and Yu-Sung Yeh

Chemical Engineering Department and Ames Laboratory-ERDA
Iowa State University
Ames, Iowa 50011

Introduction

A number of Thermochemical water splitting processes have been proposed which utilize the reverse Deacon Reaction to liberate oxygen from water. The balance of the process is devoted to liberating the hydrogen and regenerating chlorine and other reagents. The reverse Deacon reaction is a high temperature gas phase reaction.

$$H_2O + Cl_2 \rightarrow 2HCl + \tfrac{1}{2} O_2$$

The thermochemical data for this reaction are quite well documented and the free energy change is zero at about 860K. Proposals generally suggest running the reaction at 900 to 1200K with an excess of water to minimize the recycle of chlorine.

An alternate process for liberating oxygen is the pair of reactions involving magnesium compounds.

$$Mg(OH)_2 + Cl_2 \rightarrow MgCl_2 + H_2O + \tfrac{1}{2}O_2$$

$$MgCl_2 + 2H_2O \rightarrow Mg(OH)_2 + 2HCl$$

These reactions were proposed by Wentorf and Hanneman (1) of General Electric as part of one of their cycles. Note that the sum of these two reactions is the reverse Deacon reaction. Actually, these reactions are written as a condensed representation of the net effect of several reactions. The first reaction, as proposed at G. E., is run in aqueous solution and requires a catalyst to decompose an intermediate hypochlorite. Under the proper conditions nearly pure oxygen is evolved from the solution so that gas phase separation is minimized.

The second reaction in this pair is a high temperature solid-gas reaction which has been used commercially to produce MgO. One process which has been discussed in the literature (2) uses a spray tower for countercurrent contact of combustion products and water with $MgCl_2$. However, oxygen will react with HCl to regenerate chlorine, so the oxygen concentration in the combustion products must be minimized if HCl is the desired product.

A variant of this process is the use of both MgO and $MgCl_2$ in the solid phase as:

$$MgO + Cl_2 \xrightarrow{720K} MgCl_2 + \tfrac{1}{2}O_2$$

$$MgCl_2 + H_2O \xrightarrow{810K} MgO + 2HCl$$

These reactions have been suggested by Abraham (3). The free energy change for these reactions is approximately zero at the indicated temperatures. The heat of reaction at 298K are -37.6kJ and 96.3kJ, respectively.

The list of alternates to the reverse Deacon reation is essentially completed by mentioning the reactions suggested by Bowman (4):

$$Cl_2 + SO_2 + 2H_2O \rightarrow 2HCl + H_2SO_4$$

---

*Work performed for the U.S. Energy Research and Development Administration under Contract No. W-7405-eng-82.

$$H_2SO_4 \rightarrow H_2O + SO_2 + \frac{1}{2}O_2$$

The first of these reactions would be a low temperature reaction producing concentrated sulfuric acid. The high temperature decomposition of sulfuric acid has been considered as part of several sulfur based thermochemical cycles. The sulfur reactions will not be considered further in this paper.

The purpose of this paper is to present preliminary kinetic data for each of these reaction schemes and compare processing requirements. Any of the above reaction paths could be used in a thermochemical cycle which requires the chemical effect of the reverse Deacon reaction. The choice among the processes depends upon the heat balance considerations, the work of seperation and how well the process can be integrated with the rest of the cycle. Integration with a cycle is of primary importance in heat balance considerations and the recovery and reuse of HCl elsewhere in the cycle. That is, the need for a wet HCl gas, anhydrous HCl gas or aqueous solution of HCl may make one reaction scheme more attractive than another. Relative reaction rates and corrosion rates will also be important in terms of their affect on investment and maintenance costs.

Reverse Deacon Reaction

The thermochemical data for this reaction have been worked out and equilibrium compositions can be calculated reasonably accurately. Process heat balances have been reported (5) for the Mark 7 cycle and this, of course, includes the reverse Deacon reaction. The process diagram as proposed in that cycle is shown in Figure 1. Chlorine and water are fed to a reactor which operates at about 1000K. Assuming a stoichiometric feed mixture and equilibrium at the exit of the reactor, about 52% of the water and chlorine will be reacted and the HCl concentration will be about 46%. This means about 18 moles of HCl azeotrope will be circulated to the absorber for each mole of chlorine reacted. The absorber product will then be above the azeotrope composition and dry HCl can be taken from the top of the distillation coumn. The absorber offgas is then cooled to remove the remaining HCl and H_2O and the oxygen and chlorine are further cooled and compressed to separate liquid chlorine. The oxygen-chlorine compression work could be avoided by preferential absorption of chlorine in an appropriate solvent. One process has suggested sulfur monochloride as a solvent (6).

This process diagram has no provision for recovering the excess water which must be fed. Since each thermochemical cycle will have somewhat different needs for HCl and water, the best means for recycling the water will vary. Obviously, some water could be recycled from the absorber offgas condenser. The other possibility is installation of an azeotrope breaker column in the azeotrope recycle stream. Sulfuric acid is frequently used to dry an HCl-H_2O azeotrope. For purposes of comparing the reverse Deacon process with alternate processes, the recovery of the water and the source and composition of the HCl stream to be used in the thermochemical cycle are not primary consideration. That is, comparison of the oxygen liberating processes will not depend heavily on the recovery and recycle of water since most processes will have similar needs.

The kinetics of this reaction have received very little attention. Scattered literature results indicate that the uncatalyzed rate of reaction is quite slow. Catalysts for the Deacon reaction, the reverse of the reaction used here, have been developed but they are too volatile for the projected operating temperature. A patent assigned to Air Reduction Co. (6) suggests using rare earth chlorides which would seem to be reasonable Russian workers (7) have used mixtures of MgO, MgCl and CaO as catalysts, but volatility may also be a problem with these compounds. None of these workers have presented reaction rate data. Therefore, it is not known whether a catalyst will be required at the proposed operating temperature of 1000K.

To obtain preliminary reaction rate data on the reverse Deacon reaction, a simple once-through system was assembled as a plug flow reactor. The chlorine and steam feed streams were preheated and passed through a mixing zone prior to entering the reactor. The reactor temperature was maintained by a clamshell furnace controlled to ±3°C. The reactor was constructed of 6mm ID Vycor tubing about 150cm long. The reactor was constructed in five horizontal passes through the 30cm furnace. This construction was necessary to provide an adequate velocity in the reactor while obtaining sufficient residence time to give 10 to 20% conversion. The progress of the reaction was monitored by condensing H_2O and HCl in a water scrubber, reacting excess Cl_2 in a KI solution and finally collecting the O_2 in an inverted graduated cylinder. The chlorine and water flow rates were varied in each run so that the residence time in the reactor varied between 2.5 and 6.5 seconds while the ratio of water to chlorine feed concentration varied between 0.5 and 2.0.

The experiments were run at atmospheric pressure and two temperatures, 900K and 950K. The results are given in Table 1. These data were analyzed by assuming a rate equation and applying the plug flow reactor model. The general rate equation

$$r = k_1\{Cl_2\}^a\{H_2O\}^b - k_2\{HCl\}^c\{O_2\}^d \qquad 1)$$

was used where the brackets indicate concentrations in moles per liter. Since the equilibrium conversions for this reaction are greater than 40% and the measured conversions were always less than 50% of the equilibrium conversion, the reverse reaction was considered negligible. All integer combinations of a and b between 0 and 2 were used to test rate models. Values of $a=\frac{1}{2}$ with $b=o$ or 1 were also tried. A total of 12 reaction rate models were tested.

The plug flow reactor model (see e.q., 8) in the form was used to test each

$$\tau = C_{Ao}\int_o^{X_{Af}} \frac{dX_A}{r} \qquad 2)$$

rate equation. By defining X_A as the moles of chlorine reacted per mole of chlorine fed and accounting for the volume change with extent of reaction, the concentration of chlorine is $(Cl_2) = C_A = C_{Ao}(1-X_A)\frac{2(N+1)}{2(N+1)+X_A}$. Here, C_{Ao} is the feed concentration in g-moles/liter. Using these concentrations in equation 1 with $k_2=0$, substituting equation 1 into equation 2 and integrating relates the reactor exit conversion, X_{Af}, to the residence time τ and the molar water to chlorine feed ratio, N.

The model which appears to give the best fit results from using a=1, b=o in equation 1. The result in this case is

$$k_1\,\tau = -\frac{X_{Af} + (2N+3)\ln(1-X_{Af})}{2N+2} = X \qquad 3)$$

A plot of the right hand side of equation 3 versus τ will give a straight line of slope k_1 if the correct rate equation has been chosen. A plot of equation 3 is shown in Figure 2 for both the 900K and 950K experiments. The values of k_1, are 0.032 $sec.^{-1}$ at 900K and .051 sec^{-1} at 950K. Assuming on Arehnius relationship, $k_1 = Ae^{-E/RT}$, gives A=224 sec^{-1} and E=66.2 kJ.

All 12 rate expressions were similarly analyzed. With one exception, none of the other rates expressions approximated a linear relationship. The exception is the case of a=2, b=1 or $r=k_2(Cl_2)^2\,(H_2O)$ 4). Figure 3 shows the results for equation 4 when plotted in the manner corresponding to equation 3. The straight lines in Figure 3 yield the constants $k_2=880$ $(g\text{-}mole/\ell)^{-2}$ sec^{-1} at 900K, $k_2=1762$ $(g\text{-}mole/\ell)^{-2}sec^{-1}$ at 950K, E=971. kJ and $A=3.82\times10^6$.

The model shown in Figure 2 appears to give a slightly better fit of the data than the one in Figure 3, particularly at 950K. This model is also easier to justify mechanistically in that it implies that the reaction which forms chlorine radicals is

$$Cl_2 \rightleftarrows 2Cl.$$

rate controlling. The slightly greater dispersion of the data at 950K might suggest that the formation of chlorine radicals is not the only rate limitation at the higher temperature. In any event it seems obvious that these data should be used only in the range of conditions under which they were determined.

The residence time required here suggests that a catalyst would be justified to increase the reaction rate (decrease the residence time) in a commercial scale reactor operating at 900 to 950K. In that case, cooling of the reactor products would probably be rapid enough to avoid a significant amount of reverse reaction. If the reaction temperature is raised to 1100K, a catalyst may not be necessary but the initial cooling would need to be very rapid to avoid the reverse reaction. Further data are required to clarify this point.

$Mg(OH)_2$ - $MgCl_2$ Reactions

The magnesium reactions proposed by Wentorf and Hanneman (1) of General Electric were written as

$$Mg(OH)_2 + Cl_2 \rightarrow Mg\,Cl_2 + H_2O + \tfrac{1}{2}O_2$$
$$Mg\,Cl_2 + H_2O \rightarrow Mg\,(OH)_2 + 2HCl$$

Although they recognized that these reactions were not the reactions that actually occurred, they did not indicate all the potential difficulties. A more indicative, but still incomplete, reaction sequence can be written as

$$Mg\,O\,(s) + H_2O(\ell) \xrightarrow{350K} Mg\,(OH)_2(aq) \qquad \Delta H_{298} = -37.6kJ$$

$$Mg\,(OH)_2(aq) + Cl_2(g) \xrightarrow{350K} Mg\,Cl_2(aq) + H_2O(\ell) + \tfrac{1}{2}O_2(g) \qquad \Delta H_{298} = 6.3kJ$$

$$Mg\,Cl_2(aq) + 6\,H_2O(\ell) \xrightarrow{350K} Mg\,Cl_2\,6\,H_2O(s) \qquad \Delta H_{298} = -347kJ$$

$$Mg\,Cl_2\,6\,H_2O\,(s) \xrightarrow{810K} MgO\,(s) + 2HCl(g) + 5\,H_2O(g) \qquad \Delta H_{298} = 496kJ$$

All of these reactions occur quite readily. The second reaction produces an intermediate hypochlorite which must be decomposed catalytically. The addition of cobalt chloride, for example, produces a finely divided cobalt oxide which permits the hypochlorite decomposition to proceed very rapidly (9). However, this reaction will not occur in a concentrated $MgCl_2$ solution. Therefore, reaction 2 must be run in a dilute solution and the excess water must then be evaporated to crystallize $MgCl_2 \cdot 6\,H_2O$ in reaction 3. This evaporation adds substantially to the already excessive heat load for the process. The crystallization process will also remove the catalyst from solution and the catalyst would then pass through reaction 4. However, when the cobalt oxide catalyst is removed from solution and dried it becomes a less effective catalyst. Some catalyst regeneration procedure would probably be required to provide finely divided particles again for reaction 2.

The catalyst handling problems, the concentration and crystallization of $MgCl_2$ from solution and the excessive heat required to decompose the hexahydrate to MgO are each serious detriments to this process and collectively, preclude further consideration of this process as an alternate to the reverse Deacon reaction.

MgO-$MgCl_2$ Reactions

The catalyst and dehydration problems of the above reactions can be avoided by running solid-gas reactions written as

$$MgO\,(s) + Cl_2(g) \xrightarrow{720K} Mg\,Cl_2(s) + \tfrac{1}{2}O_2(g) \qquad \Delta H_{298} = -37.6RJ$$

$$Mg\,Cl_2(s) + H_2O(g) \xrightarrow{810K} MgO\,(s) + 2HCl\,(g) \qquad \Delta H_{298} = 96.3RJ$$

magnesium compounds on a porous surface and alternately passing steam and chlorine over the bed. The use of two beds in much the same way as ion exchange resins are used would provide a semi-continuous process. The data presently available indicates that no other process using the magnesium reactions is an alternative to the reverse Deacon reaction.

Conclusions

The reverse Deacon reaction is shown to require very high temperatures (1100K or higher) or a catalyst to obtain satisfactory reaction rates. If a high temperature is used, the reverse reaction is likely to occur as the products are cooled. The reverse reaction could be minimized by very rapid cooling but this would incur irreversible heat losses in addition to the heat required to drive the reaction. The work of separation and recycle is also very large for this reaction.

Preliminary experimental work on the chlorination of magnesia and the hydrolysis of magnesium chloride indicates that both these reactions must be run as solid gas reactions. In addition, they must be run in such a way that diffusional limitations to the reaction rate are avoided. Successful demonstration of such a process may lead to a good alternate to the reverse Deacon reaction.

REFERENCES

1. Wentorf, R. H., and Hanneman, R. E. Science, 185, No. 4148, 311 (July, 1974).

2. Hoppe, H. and Maurer, B. Chem. Techn., 18, No. 5, 257 (May, 1966).

3. Abraham, B. M. and Schreiner, F. I&EC Fund., 13, No. 4, 305 (Nov., 1974).

4. Bowman, M. G., Los Alamos Scientific Laboratory, Private Communication.

5. Euratom, Joint Nuclear Research Centr., Ispra. EUR 5059e Progress Report No. 3, 1973.

6. Johnstone, H. F. CEP, 44, No. 9, 657 (Sept., 1948).

7. Shelud'ko, M. K. Ukrain. Khem. Zhur., 9, 410 (1934).

8. Levenspeil, O. Chemical Reation Engineering, Wiley, 1967.

9. Ulrichson, D. L. and Powers, E. J., Paper presented to Miami Hydrogen Energy Conference, March, 1975.

10. Fr. Patent 1,399,518. May 14, 1965, Asahi Glass Co. Ltd, Japan.

11. Vilnyansky, Ya. E. and Savinkova, E. I. Journal of Applied Chem. of the USSR, 26, No. 7, 735 (July, 1953).

12. Kelley, K. K. U.S. Dept. of Int., Bureau of Mines, Technical Paper, 676, (1945).

13. Barin and Knacke, Thermochemical properties of inorganic substances, Springer-Verlag, N.Y., 1973.

14. Vilnyansky, Y., E. and Savinkova, E. I. Journal of Applied Chem. of the USSR, 28, No. 8, 827 (August, 1955).

15. Aman, J. Bull. Res. Counc. of Israel, Vol. 5C, 108 (1955).

16. Doerner, H. A. and Holbrook, W. F., Chlorination of Magnesia, Report of Investigations, U.S. Bureau of Mines, Publication R.I. 3833, 1945.

17. da Cunha, O. G. C., Metallurgia, Vol. 29, No. 188, pp.425-431, 1973. Translated for Ames Laboratory, ERDA.

Table 1
Experimental Results

Run Number	Feed Rate* (c.c./min)	$(Cl_2)X10^3$ (g-moles/l)	$(H_2O)X10^3$ (g-moles/l)	N	τ (Sec.)	Conversion (%)
A 1	847	5.823	7.727	1.327	2.41	6.91
A 2	725	4.523	9.027	1.996	2.81	7.88
A 3	847	5.823	7.727	1.327	2.41	6.91
A 4	725	4.523	9.027	1.996	2.81	7.06
A 5	550	6.559	6.991	1.066	3.71	9.24
A 6	611	7.258	6.292	0.867	3.34	8.16
A 7	550	6.559	6.991	1.066	3.71	9.24
A 8	611	7.258	6.292	0.867	3.34	8.20
A 9	780	6.327	7.223	1.141	2.62	8.34
A 10	658	4.987	8.563	1.717	3.10	10.77
A 11	780	6.327	7.223	1.141	2.62	8.31
A 12	658	4.987	8.563	1.717	3.10	10.59
A 13	463	4.523	9.028	1.996	4.41	13.82
A 14	495	5.108	8.442	1.653	4.12	14.29
A 15	532	5.691	7.859	1.381	3.84	14.13
A 16	574	6.276	7.274	1.159	3.55	13.60
A 17	636	6.976	6.574	0.942	3.21	12.06
A 18	550	5.958	7.592	1.274	3.71	13.62
A 19	471	4.450	9.102	2.046	4.33	9.48
A 20	503	5.030	8.520	1.694	4.06	11.87
A 21	539	5.610	7.941	1.416	3.78	11.20
A 22	582	6.193	7.357	1.188	3.50	12.38
A 23	643	6.893	6.657	0.966	3.17	10.81
A 24	313	6.695	6.855	1.024	6.52	17.50
A 25	345	7.333	6.217	0.848	5.92	16.90
A 26	382	7.931	5.619	0.708	5.35	14.76
A 27	424	8.498	5.052	0.594	4.81	13.46
A 28	486	9.135	4.415	0.483	4.20	12.12
B 1	332	6.365	6.472	1.017	6.14	21.96
B 2	364	6.938	5.898	0.850	5.60	23.28
B 3	403	7.505	5.332	0.710	5.06	24.00
B 4	448	8.043	4.794	0.596	4.55	23.15
B 5	513	9.127	4.423	0.485	3.98	21.15
B 6	398	5.317	7.520	1.414	5.13	19.61
B 7	430	5.882	6.955	1.182	4.74	20.33
B 8	469	6.457	6.380	0.988	4.35	20.55
B 9	514	7.018	5.819	0.829	3.97	20.23
B 10	579	7.668	5.169	0.674	3.52	17.94
B 11	441	4.792	8.044	1.678	4.62	18.69
B 12	474	5.341	7.496	1.403	4.31	20.22
B 13	512	5.908	6.928	1.173	3.98	18.54
B 14	558	6.470	6.366	0.984	3.66	17.24
B 15	622	7.132	5.705	0.800	3.28	15.64
B 16	479	4.412	8.424	1.909	4.26	19.87
B 17	512	4.944	7.892	1.596	3.99	19.89
B 18	550	5.500	7.336	1.334	3.71	19.27
B 19	596	6.058	6.779	1.119	3.42	18.54
B 20	660	6.721	6.116	0.910	3.09	16.14

*A-Group are based on 900°K
B-Group are based on 950°K

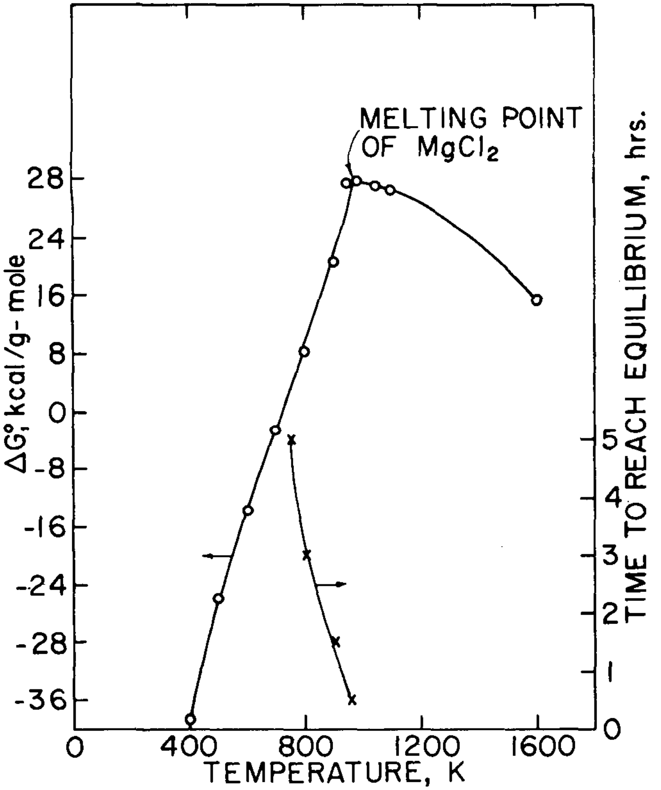

Figure 4

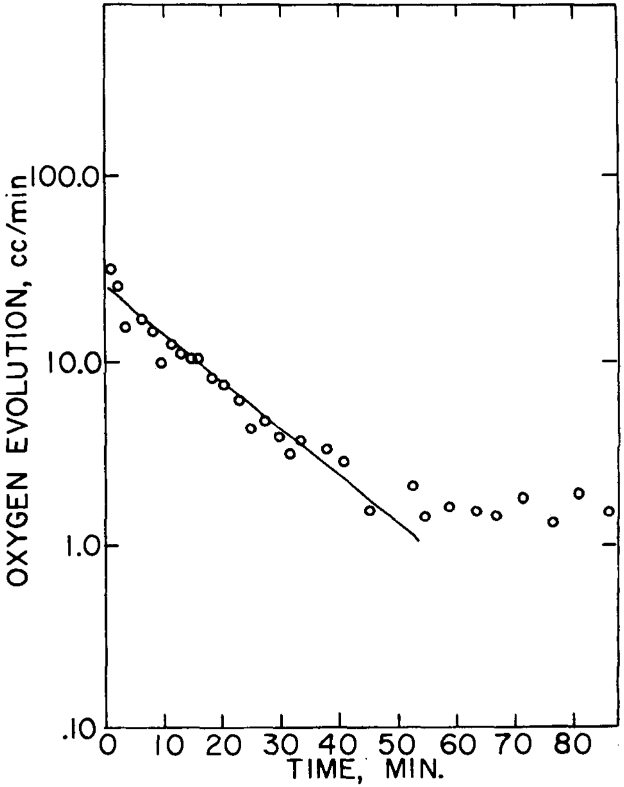

Figure 5

TECHNICAL STATUS OF THE WESTINGHOUSE SULFUR CYCLE FOR THE THERMOCHEMICAL DECOMPOSITION OF WATER, L.E. Brecher, S. Spewock, C.J. Warde, Westinghouse Research Laboratories.

The Westinghouse sulfur cycle is described in some detail. Kinetic results, catalyst effectiveness and life test results, and a study of techniques to insure a current efficiency of 100% for hydrogen production are described.